



Identifying trend nature in time series using autocorrelation functions and R-routines based on stationarity tests

M Boutahar, M Royer-Carenzi

► To cite this version:

M Boutahar, M Royer-Carenzi. Identifying trend nature in time series using autocorrelation functions and R-routines based on stationarity tests. *International Journal of Computational Economics and Econometrics*, 2024, 14 (1), pp.1 - 22. hal-03468714v2

HAL Id: hal-03468714

<https://hal.science/hal-03468714v2>

Submitted on 9 Apr 2024

HAL is a multi-disciplinary open access archive for the deposit and dissemination of scientific research documents, whether they are published or not. The documents may come from teaching and research institutions in France or abroad, or from public or private research centers.

L'archive ouverte pluridisciplinaire **HAL**, est destinée au dépôt et à la diffusion de documents scientifiques de niveau recherche, publiés ou non, émanant des établissements d'enseignement et de recherche français ou étrangers, des laboratoires publics ou privés.

Identifying trend nature in time series using autocorrelation functions and stationarity tests

M. Boutahar^a and M. Royer-Carenzi^a

^aAix Marseille Univ, CNRS, Centrale Marseille, I2M, UMR 7373, Marseille, France

Abstract

Time series non-stationarity can be detected thanks to autocorrelation functions. But trend nature, either deterministic or either stochastic, is not identifiable.

Strategies based on Dickey-Fuller unit root-test are appropriate to choose between a linear deterministic trend or a stochastic trend. But all the observed deterministic trends are not linear, and such strategies fail in detecting a quadratic deterministic trend. Being a confounding factor, a quadratic deterministic trend makes appear a unit root spuriously.

We provide a new procedure, based on Ouliaris-Park-Phillips unit root test, convenient for time series containing polynomial trends with degree higher than one. Our approach is assessed on simulated data.

The strategy is finally applied on two real datasets : money Stock in USA and also on CO2 atmospheric concentration. Compared with Dickey-Fuller diagnosis, our strategy provides the model with the best performances.

Keywords: time series; stationarity; autocorrelation functions; unit root tests; Dickey-Fuller; KPSS; OPP test; trend detection; deterministic or stochastic trend; quadratic trends involve spurious unit root.

1. Introduction

Time series non-stationarity can originate from various sources: either from a trend component or from a seasonal or even a cyclical component. In this paper, we will be interested in the non-stationarity caused by a trend. There are two kinds of trends: either a deterministic trend which can be modeled by some function of time (polynomial trend is generally considered), or a stochastic trend which presents unit roots. Deterministic and stochastic trends are two specific models suggested by Nelson and Plosser in [19].

$$\text{Deterministic trend (Det,d)} \quad Z_t = a_0 + a_1 t + \dots + a_d t^d + B_t \quad (1)$$

$$\text{Stochastic trend (Sto,d)} \quad \Delta^d(Z_t) = B_t, \quad (2)$$

where d is an integer and $a_d \neq 0$. Moreover, L is the backshift operator, i.e. $LZ_t = Z_{t-1}$, so that the 1-lag difference operator Δ can be expressed as

$$\Delta(Z_t) = (1 - L)(Z_t) = Z_t - Z_{t-1}.$$

Finally $(B_t)_t$ is a moving average process

$$B_t = \sum_{j \in \mathbb{Z}} b_j \mathcal{E}_{t-j}, \quad (\text{H1})$$

where $(\mathcal{E}_t)_t$ is a sequence of identically distributed and independent centered variables, such that

$$E(\mathcal{E}_t^{2k}) < \infty, \text{ for some } k \geq 2, \quad (\text{H2})$$

and where parameters b_j ($j \in \mathbb{Z}$) satisfy

$$\begin{aligned} \sum_{j \in \mathbb{Z}} |b_j| < \infty & \quad \sum_{j \in \mathbb{Z}} b_j \neq 0 & \quad \sum_{j \in \mathbb{Z}} b_j^2 |j| < \infty. \end{aligned} \quad (\text{H3})$$

(H3-a)
(H3-b)
(H3-c)

We denote $(B_t)_t$ as **(SN)**, for *Stationary Noise*. It's well known that causal and invertible ARMA pocesses satisfy Hypotheses (H1) and (H3). When $B_t = \mathcal{E}_t$, it is called **(WN)** for *white noise*. In this case, the associated models defined in Equations (1) and (2), are referred as **(Det_W,d)** and **(Sto_W,d)**.

When modeling time series, specially for macroeconomic and financial data, it is very important to identify the nature of the trend: either deterministic or stochastic. Indeed, every type of trend induces specific behaviors, that we can illustrate with moments properties. Let us consider a **(Det,1)** then $\mathbb{E}(Z_t) = a_0 + a_1 t$, and $\text{var}(Z_t) = \sigma_B^2$, providing a stationary variance but a non-stationary mean. On the contrary, under a **(Sto,1)** model with $Z_0 = 0$, we have $\mathbb{E}(Z_t) = 0$, and $\text{var}(Z_t) = t\sigma_B^2$, providing the opposite feature. Thus the source of non-stationarity differs with trend nature. Consequently identifying the correct trend is fundamental. Globally, time series with a deterministic trend always revert to the trend in the long run (the effects of shocks are eventually eliminated); and the prediction intervals have constant width. On the contrary, time series with a stochastic trend never recover from shocks to the mean (the effects of shocks are permanent); and the forecast confident intervals grow with the horizon. Several authors (see for instance [6] and [18]) studied the consequences of an inappropriate modeling choice, underlying the importance of developing procedures able to produce a reliable classification.

Note that non stationarity coming from a periodical trend (seasonal or even a cyclical) can also be considered. One can consider the following models:

$$\text{Deterministic seasonality} \quad Z_t = \mathbf{S}_t + Y_t, \quad (3)$$

$$\text{Stochastic seasonality} \quad \Delta_r^D(Z_t) = Y_t, \quad (4)$$

where Y_t has a trend, which can be modeled by either model (1) or (2). Moreover, in (3), we define $\mathbf{S}_t = S_i$ if $(t \bmod r) = i$, and S_1, \dots, S_r are the seasonal components. And in (4), we consider the seasonal difference operator (r -lag difference operator)

$$\Delta_r(Z_t) = (1 - L^r)(Z_t) = Z_t - Z_{t-r},$$

where r is the season assumed to be known and D is an integer.

Autocorrelation function properties have been widely studied, and are helpful to specify accurate models for stationary time series. The theoretical autocorrelation function at lag h ($|h| < n$)

is estimated from data (Z_1, \dots, Z_n) with the random variable

$$\Xi(h) = \frac{\sum_{t=1}^{n-h} (Z_{t+h} - \bar{Z})(Z_t - \bar{Z})}{\sum_{t=1}^n (Z_t - \bar{Z})^2}, \quad (5)$$

where

$$\bar{Z} = \frac{\sum_{t=1}^n Z_t}{n},$$

is the random mean. We show that autocorrelation functions also have interesting properties in our framework, since they permit to identify the presence of a trend in a time series. Nevertheless it can not be used to distinguish between either a deterministic or a stochastic trend.

Dickey and Fuller developed a unit root test that is an essential tool in time series modeling [11]. The authors considered the following models

$$\begin{aligned} \mathbf{M}_1 : Z_t &= \rho Z_{t-1} + \mathcal{E}_t \\ \mathbf{M}_2 : Z_t &= a_0 + \rho Z_{t-1} + \mathcal{E}_t \\ \mathbf{M}_3 : Z_t &= a_0 + a_1 t + \rho Z_{t-1} + \mathcal{E}_t, \end{aligned}$$

where $(\mathcal{E}_t)_t$ is a white noise. Dickey-Fuller procedure permits to test the null hypothesis of a unit root ($\rho = 1$) against the alternative hypothesis of a stationary AR(1) model without drift (resp. with drift, resp. with trend), accordingly to model \mathbf{M}_1 (resp. \mathbf{M}_2 , resp. \mathbf{M}_3). Note that a time series with a (linear) deterministic trend, as defined in $(\mathbf{Det}_W, \mathbf{1})$, is included in \mathbf{M}_3 model, by taking $\rho = 0$. Consequently, under a (linear) deterministic trend, Dickey-Fuller unit-root test, led in \mathbf{M}_3 framework, usually rejects the null hypothesis. On the other hand, $(\mathbf{Sto}_W, \mathbf{1})$ -time series are included in \mathbf{M}_1 model, with $\rho = 1$, so that (\underline{H}_0) , tested in \mathbf{M}_1 framework, is usually not rejected, accordingly with the rejection rate.

Several strategies based on Dickey-Fuller unit root-test have been developed ([10, 21, 12]), and they mostly appear to be appropriate to choose between a linear deterministic trend or a stochastic trend. But all the observed deterministic trends are not linear, trends with higher degrees can be involved. In this case, Ertur noticed in [13] that the usual strategies fail in detecting a quadratic deterministic trend. Indeed, under a quadratic trend for instance, Dickey-Fuller test generally concludes to the presence of a (spurious) unit root, even using model \mathbf{M}_3 that allows a linear trend.

In this paper, we aim to include polynomial trends with a degree higher than one. Let us introduce the general model :

$$\mathbf{M}_{3,d} : Z_t = a_0 + a_1 t + \dots + a_d t^d + \rho Z_{t-1} + B_t \quad (a_d \neq 0).$$

In [20], Ouliaris, Park and Phillips developed a test that corrects the bias caused by high degree trend when testing for a unit root. We included this test in a strategy, that correctly identifies either a deterministic trend or a stochastic one.

In Section 2, we detail autocorrelation functions convergence when time series are driven by a trend, either deterministic or stochastic. This result permits to detect the presence of a trend, but without precise identification. We also study existing strategies based on Dickey-Fuller tests, and analyze their performance in classifying models $(\mathbf{Det}_W, \mathbf{1})$, $(\mathbf{Det}_W, \mathbf{2})$, $(\mathbf{Sto}_W, \mathbf{1})$

and **(Sto_W,2)**. Note that we also consider the simplest model **(WN)** as a null-model. Next, we provide a new strategy, based on Trend Diagnosis Tests (TDT), theoretically able to identify trends type, even when higher-degrees d are considered. In this paper we study the asymptotic behavior of autocorrelation functions only for models (1) and (2). Similar results can be obtained for models (3) and (4) but are out of the scope of this paper. However, to deal with seasonal data (monthly, quarterly or biannual) one can extract the seasonal component first and then apply our proposed strategy. In Section 3, we ran simulations of processes generated by models **(WN)**, **(Det_W,1)**, **(Det_W,2)**, **(Sto_W,1)** such as **(Sto_W,2)** and we applied the various tests of stationarity studied previously. It appears that the Dickey-Fuller tests fail in the presence of a degree 2 trend. On the other hand, the tests included in our TDT strategy behave as expected on simulations even when **(WN)** is replaced by a **(SN)** underlying process. But because of Type I of Type II errors associated with the different tests, the simulations also reveal responses that are complementary to the theoretical one. This provides a modeling suggestion when the series does not produce one of the theoretical responses. Finally, in Section 4, we apply our strategy on real data such as Money Stock in USA and also on the CO2 atmospheric concentration, that includes a monthly seasonal component. All the functions are implemented in **R** language, and they are available at the website:

www.i2m.univ-amu.fr/perso/manuela.royer-carezzi/AnnexesR.TrendTS/TrendTS.html

2. Trend detection and nature identification

2.1. Detection with autocorrelation functions

It is essential to start by plotting the graph of the series in order to visualize its evolution, but the presence or absence of a trend is sometimes difficult to detect from the plot. Autocorrelation appears to be a powerful tool in the detection of a trend insofar as its behavior is specific in the presence of a trend. We recall that theoretical autocorrelations $\rho(h) = \text{cor}(Z_t, Z_{t+h})$ are well-defined only if process $(Z_t)_t$ is square-integrable and stationary. However the associated random variables $\Xi(h)$, as defined in Equation (5), can be computed for any observed time series (Z_1, \dots, Z_n) .

2.1.1. Autocorrelation functions behavior for **(WN)**-time series

Theorem 2.1.

Let $(Z_t)_t$ be a white noise. Then

$$\sqrt{n} {}^t(\Xi(1), \Xi(2), \dots, \Xi(r)) \xrightarrow[n \rightarrow +\infty]{\mathcal{L}} \mathcal{N}_r({}^t(0, \dots, 0), Id_r),$$

where tv denotes the transpose of vector v , and Id_r is the identity $r \times r$ -matrix.

Theorem 2.1 is a particular case of Theorems 7.2.1. or 7.2.2. in [4], that require Hypotheses (H1), (H3-a) and either Hypothesis (H2) or (H3-c). Thus, we get that the random variables $\Xi(1), \Xi(2), \dots, \Xi(r)$ are asymptotically independent and identically distributed as Gaussian random variables with zero mean and variance $1/n$. Consequently, for any fixed lag $h = 1, \dots, r$, for large n , the sample autocorrelation function $\sqrt{n} \hat{\rho}(h)$ is expected to be a realization of a standard Gaussian, that is to be valued in the interval $[-1.96, 1.96]$, with 95% coverage. Thus, sample autocorrelation functions (acf) are used to assess for white noise. But even when the underlying process is a white noise, several autocorrelations among $\hat{\rho}(1), \dots, \hat{\rho}(r)$ may lie out of the interval $[-1.96/\sqrt{n}, 1.96/\sqrt{n}]$. The asymptotic independence property for variables $\Xi(h)$ implies that, when sample size n is large, the number of observed autocorrelation functions out of this interval behaves as a Binomial $\mathcal{B}(r, 0.05)$ distribution. We take into account the multiple

testing paradigm, on the one hand by incorporating the binomial exact test and on the other hand by incorporating a global testing procedure, using Sidak correction . As an example, we simulate a white noise, and compute sample autocorrelation functions. Figure 1 shows that 3 values lie out of the interval $[-1.96/\sqrt{n}, 1.96/\sqrt{n}]$, plotted with blue dashed lines. But binomial exact test (p-value = 0.1159) confirms that such a number remains consistent with white noise hypothesis. Moreover, a second set of interval, computed with Sidak correction, is provided, and plotted with red dotted lines. If at least one sample autocorrelation function lies out this global interval, then white noise hypothesis is rejected. In our simulation, white noise diagnosis is confirmed, both by graphics and by Binomial's test.

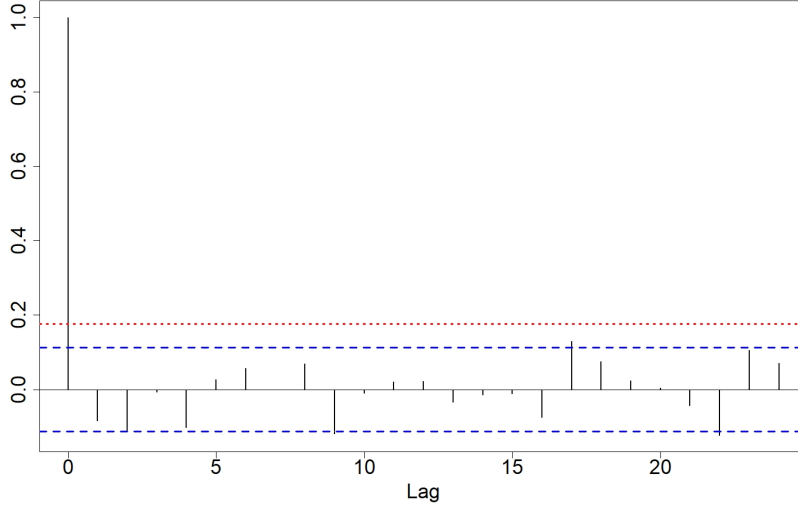


Figure 1.: Sample autocorrelation functions for a white noise simulation.

2.1.2. Autocorrelation functions for $(\mathbf{Det}, \mathbf{d})$ -time series

Theorem 2.2.

Let $(Z_t)_t$ be a stochastic process such that $Z_t = \sum_{j=0}^d a_j t^j + B_t$, where $a_d \neq 0$ and $(B_t)_t$ is (\mathbf{SN}) satisfying Hypotheses (H1) to (H3). Then

$$\Xi(h) \xrightarrow[n \rightarrow +\infty]{\mathbb{P}} 1, \quad \forall h \neq 0.$$

Proof is given in Appendix A. Figure 2 (Left) illustrates the slow decreasing behavior of sample autocorrelation functions when time series are driven by a deterministic $(\mathbf{Det}, \mathbf{2})$ trend.

2.1.3. Autocorrelation functions for $(\mathbf{Sto}_W, \mathbf{d})$ -time series

Theorem 2.3.

Let $(Z_t)_t$ be a stochastic process such that $\Delta^d(Z_t) = \mathcal{E}_t$, with $Z_t = 0$, for any $t \leq 0$ and $(B_t)_t$ is (\mathbf{SN}) satisfying Hypotheses (H1) to (H3). Then

$$\Xi(h) \xrightarrow[n \rightarrow +\infty]{\mathbb{P}} 1, \quad \forall h \neq 0.$$

Proof is given in Appendix B. Figure 2 (Right) illustrates the slow decreasing behavior of sample autocorrelation functions when time series are driven by a stochastic (**Sto**_W,**2**) trend.

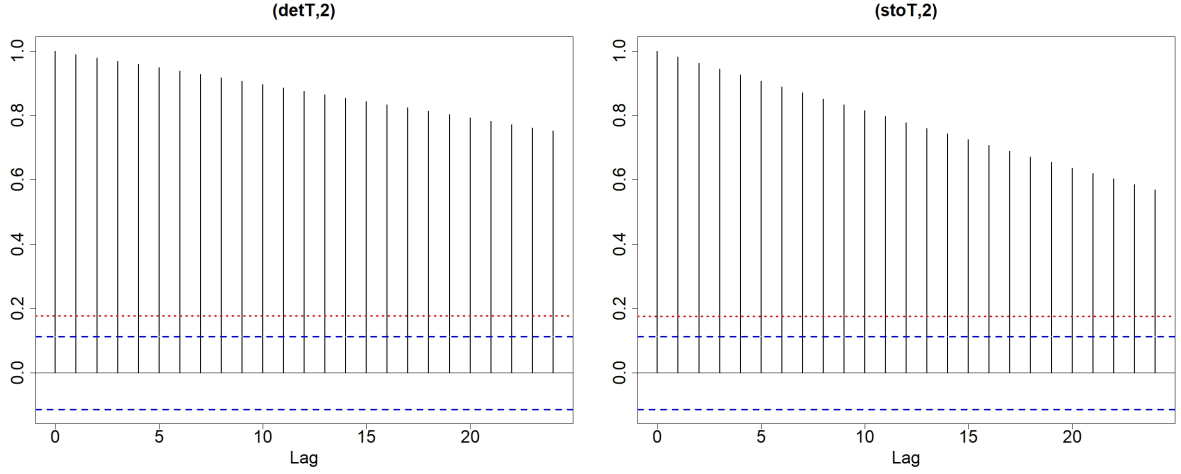


Figure 2.: Sample autocorrelation functions for simulations with either a deterministic (Left) or a stochastic trend (Right).

2.2. Trend-nature identification with stationarity tests

Previously, we showed that the autocorrelation functions, computed from variables Z_1, \dots, Z_n , have a particular asymptotic behavior in presence of a trend. But Figure 2 illustrates that the behavior is similar either for a deterministic or a stochastic trend. Consequently, a deeper study has to be led in order to specify the type of trend.

2.2.1. Data generating process

We explore stationarity tests diagnosis according to several data generating processes, and we will also explore the associated differenced processes. We set $(B_t)_t$ a stationarity noise constructed from a white noise $(\mathcal{E}_t)_t$ with variance $\sigma_{\mathcal{E}}^2$. We consider processes $(Z_t)_t$ successively driven by one of the following models :

$$\text{(SN)} \quad Z_t = B_t \quad \implies \quad \Delta(Z_t) = B_t - B_{t-1}, \quad (6)$$

$$\text{(Det,1)} \quad Z_t = a_0 + a_1 t + B_t \quad \implies \quad \Delta(Z_t) = a_1 + B_t - B_{t-1}, \quad (7)$$

$$\text{(Det,2)} \quad Z_t = a_0 + a_1 t + a_2 t^2 + B_t \quad \implies \quad \Delta(Z_t) = a_1 + 2a_2 t + B_t - B_{t-1}, \quad (8)$$

$$\text{(Sto,1)} \quad Z_t = Z_{t-1} + B_t \quad \implies \quad \Delta(Z_t) = B_t, \quad (9)$$

$$\text{(Sto,2)} \quad Z_t = 2Z_{t-1} - Z_{t-2} + B_t \quad \implies \quad \Delta(Z_t) = \Delta(Z_{t-1}) + B_t. \quad (10)$$

Some of the previous processes are stationary while others are not. We recall that a process containing a unit root is not stationary. Thus models (**Sto,1**) and (**Sto,2**) do contain a unit root and hence are not stationary, whereas models (**Det,1**) and (**Det,2**) are not stationary although they do not contain any unit root. Table 1 indicates which of these series or differentiated series is stationary or has a unit root.

Table 1.: Stationarity and presence of a unit root for processes generated by models **(SN)**, **(Det,1)**, **(Det,2)**, **(Sto,1)** such as **(Sto,2)**, and for the associated differenced processes.

Property	DGP ^a				
	(SN)	(Det,1)	(Det,2)	(Sto,1)	(Sto,2)
Stationarity for Z_t	Yes	No	No	No	No
Stationarity for $\Delta(Z_t)$	Yes	Yes	No	Yes	No
Unit root for Z_t	No	No	No	Yes	Yes
Unit root for $\Delta(Z_t)$	No	No	No	No	Yes

^aData Generating Process.

2.2.2. Dickey-Fuller tests

In [11], Dickey and Fuller introduced unit root tests adapted to models **M₁**, **M₂** and **M₃**. Every time the null and the alternative hypothesis are mathematically expressed in the same way:

$$(\underline{H}_0) : \rho = 1 \text{ against } (\underline{H}_1) : |\rho| < 1.$$

But the alternative hypothesis interpretation depends on the considered model.

- (**M₁**) $(\underline{H}_1) : (Z_t)_t \text{ is a stationary and centered } AR(1) \text{ process;}$
- (**M₂**) $(\underline{H}_1) : (Z_t)_t \text{ is a stationary not-centered } AR(1) \text{ process;}$
- (**M₃**) $(\underline{H}_1) : (Z_t)_t \text{ is (linear-)trend stationary (TS).}$

And test statistics do not have the same expression, possibly leading to opposing conclusions, even on the same data. To distinguish between the null or the alternative hypothesis, one has to use the suitable test statistics, adapted to every model.

In [11], Dickey and Fuller also developed joined tests :

- Test Φ_1 under (**M₂**) $(\underline{H}_0) : (a_0, \rho) = (0, 1);$
- Test Φ_2 under (**M₃**) $(\underline{H}_0) : (a_0, a_1, \rho) = (0, 0, 1);$
- Test Φ_3 under (**M₃**) $(\underline{H}_0) : (a_0, a_1, \rho) = (a_0, 0, 1).$

Models **(Sto_W,1)** and **(Sto_W,2)** do contain a unit root and hence are not stationary, whereas models **(Det_W,1)** and **(Det_W,2)** are not stationary although they do not contain any unit root. Logically, Dickey-Fuller test should not reject the null hypothesis for almost realizations driven from models **(Sto_W,1)** and **(Sto_W,2)**, precisely with a rate $(1 - \alpha)\%$, where α stands for the significance level. Reciprocally, under **(Det_W,1)** and **(Det_W,2)** models, the null hypothesis should be rejected.

2.2.3. OPP stationarity test

In [20], Ouliaris, Park, and Phillips generalized Dickey-Fuller unit-root tests ρ to models **M_{3,d}** with polynomial trends, where $d = 2, 3, 4$ or 5 . We denote this general test by OPP. Note that the invariance principle for partial sums, required in OPP test, applies to **(SN)** stationary linear processes satisfying Hypotheses (H1) to (H3).

From Table 1, we guess that OPP test should reject the null hypothesis only for models **(Det,1)** and **(Det,2)**, vice versa for **(Sto,1)** and **(Sto,2)**. Applied to the differentiated series, OPP test should not reject the null hypothesis only for realizations initially driven from models **(Sto,2)**.

2.2.4. KPSS stationarity test

In [17], Kwiatkowski, Phillips, Schmidt and Shin developed another type of stationarity test, associated to an underlying **(SN)**. Contrary to Dickey-Fuller and OPP tests, KPSS test takes the presence of unit root as the alternative hypothesis, and the stationarity as the null hypothesis. Actually, KPSS test can consider as null-hypothesis either level-stationarity or trend-stationarity (stationarity around a linear deterministic trend). However, there is no extension in the literature of KPSS test considering stationarity around a polynomial deterministic trend.

Note that none model is stationary, except the simplest model **(SN)**. Hence KPSS test does not appear to be a good candidate for trend-nature identification. Nonetheless, KPSS test may reveal heterogeneous behaviors when applied to the differentiated series $\Delta(Z_t)$. Indeed, processes (Z_t) driven from models **(Det,1)** and **(Sto,1)** do become stationary as soon as they are differentiated.

Here we will use the level stationarity. Note that KPSS test does not include the case of series with non-invertible noise, as is the case for the **(SN)** and **(Det,1)** differentiated series. But it is possible to determine the nature of the convergence of the test statistic in these particular cases (see Appendix C.1.), and we even identify the behavior of the test statistic under an alternative such as a **(Det,1)** or a **(Det,2)** process (see Appendix C.2.).

2.2.5. TDT strategy

2.2.5.1. Description and theoretical diagnosis.

We introduce a strategy to identify trend nature by applying the following tests successively :

- i) OPP test to series Z_t ;
- ii) OPP test to series $\Delta(Z_t)$;
- iii) KPSS test to series Z_t ;
- iv) KPSS test to serie $\Delta(Z_t)$.

We call Trend Diagnosis Tests (TDT) the set of responses to tests **i)** to **iv)** computed on a time series. Let us denote by **Null**, the case where the null hypothesis can not be rejected, and by **Alt** otherwise. From Equations (6) to (10), we provide the theoretical response obtained by applying the TDT strategy for the following five models:

$$\text{(SN)} \quad \text{theoretical response :} \quad \mathbf{Alt/Alt/Null/Null} , \quad (11)$$

$$\text{(Det,1)} \quad \text{theoretical response :} \quad \mathbf{Alt/Alt/Alt/Null} , \quad (12)$$

$$\text{(Det,2)} \quad \text{theoretical response :} \quad \mathbf{Alt/Alt/Alt/Alt} , \quad (13)$$

$$\text{(Sto,1)} \quad \text{theoretical response :} \quad \mathbf{Null/Alt/Alt/Null} , \quad (14)$$

$$\text{(Sto,2)} \quad \text{theoretical response :} \quad \mathbf{Null/Null/Alt/Alt} . \quad (15)$$

For example the **(SN)** model does not contain unit root, and is stationary (see Table 1). So is $\Delta(\text{SN})$. Hence the OPP test will accept the alternative of no unit root for **(SN)** and $\Delta(\text{SN})$, then we have the two responses **Alt/Alt/**. On the other hand the KPSS test will accept the null hypothesis of stationarity for **(SN)** and $\Delta(\text{SN})$; then we have the two responses **/Null/Null**. Therefore the theoretical response of the TDT strategy for the **(SN)** model will be **Alt/Alt/Null/Null**. A similar explanations can be made for the other models to obtain the theoretical responses of the TDT strategy.

2.2.5.2. More diagnosis expected for simulations.

Note that, when applying the TDT strategy to a given DGP, there are sixteen possible responses; one response is the theoretical one, as given in Equations (11)-(15), whereas the other responses are not the accurate ones. For example if the DGP is (SN) model, then the expected response will be the theoretical one **Alt/Alt/Null/Null**, and the wrong responses are **w/x/y/z** where **w,x,y,z** can take either **Alt** or **Null**, except the case **w=Alt, x=Alt, y=Null, z=Null**. We insist on the fact that when applying the TDT procedure on a simulation, the observed diagnosis will not systematically be the theoretical one. Indeed, a statistical test, even a well-calibrated and powerful one, produces erroneous responses, in proportion to Type I and Type II errors. Most often, the power of a test is difficult to calculate, but when the null hypothesis is verified, the null hypothesis is still rejected in $\alpha\%$ of cases, where α is the nominal level.

- Thus when we consider for example a (WN) model, only the last two tests **iii)** and **iv)** are performed under the Null hypothesis of stationarity. But we point out that KPSS test was developed under a white noise hypothesis, that is clearly convenient for the initial series, but no longer valid for the differentiated series. Consequently, KPSS behavior in test **iii)** will be convenient, whereas KPSS behavior in test **iv)**, *i.e.* on the differentiated series, which is nothing else than a non-invertible MA(1) process, will not necessarily be in adequacy with the proportions α and $1 - \alpha$. Actually, we proved in Appendix C.1., Equation (C2), that KPSS test will never reject the null hypothesis, as n tends to ∞ , for series $(\Delta(Z_t))_t$ when $(Z_t)_t$ is (WN). Consequently, we expect, except for size distortion effect, that

$$\begin{aligned}
95\% \times 100\% &= 95\% & \text{(WN)-simulations with response} & \text{-/-/Null/Null} \\
95\% \times 0\% &= 0\% & \text{(WN)-simulations with response} & \text{-/-/Null/Alt} \\
5\% \times 100\% &= 5\% & \text{(WN)-simulations with response} & \text{-/-/Alt/Null} \\
5\% \times 0\% &= 0\% & \text{(WN)-simulations with response} & \text{-/-/Alt/Alt}
\end{aligned} \tag{16}$$

- In the same way, for a (**Det_W,1**), none of the tests **i)** to **iii)** is performed under the null hypothesis. And for test **iv)**, it is the same as applying the KPSS test on a non-invertible MA(1) process. We recall that we proved in Appendix C.1., Equation (C2), that KPSS test will never reject the null hypothesis, as n tends to ∞ , for series $(\Delta(Z_t))_t$ when $(Z_t)_t$ is (**Det_W,1**). Moreover, we proved in Appendix C.2., Equation (C3), that KPSS test will always reject the null hypothesis, as n tends to ∞ , for series under a (**Det_W,1**) model, meaning that KPSS test has a very high power (probability of rejecting the null when the alternative is true) in this case. Hence both tests **iii)** and **iv)** have a tractable behavior. Consequently, we expect, except for size distortion effect, that

$$\begin{aligned}
0\% \times 100\% &= 0\% & \text{(\textbf{Det}_W,1)-simulations with response} & \text{-/-/Null/Null} \\
0\% \times 0\% &= 0\% & \text{(\textbf{Det}_W,1)-simulations with response} & \text{-/-/Null/Alt} \\
100\% \times 100\% &= 100\% & \text{(\textbf{Det}_W,1)-simulations with response} & \text{-/-/Alt/Null} \\
100\% \times 0\% &= 0\% & \text{(\textbf{Det}_W,1)-simulations with response} & \text{-/-/Alt/Alt}
\end{aligned} \tag{17}$$

- For model (**Det_W,2**), none of the tests **i)** to **iv)** is performed under the null hypothesis. But once again, KPSS behavior is tractable both on $(Z_t)_t$ and $(\Delta(Z_t))_t$ processes. Indeed, in Appendix C.2., Equation (C3), we showed that KPSS test will always reject the null hypothesis, as n tends to ∞ , for series $(Z_t)_t$ and $(\Delta(Z_t))_t$ when $(Z_t)_t$ is generated under a (**Det_W,2**) model, meaning that KPSS test has a very high power in both cases.

Consequently, we expect, except for size distortion effect, that

$$\begin{aligned}
0\% \times 0\% &= 0\% & (\mathbf{Det}_W, \mathbf{2})\text{-simulations with response} & \text{-/-/Null/Null} \\
0\% \times 100\% &= 0\% & (\mathbf{Det}_W, \mathbf{2})\text{-simulations with response} & \text{-/-/Null/Alt} \\
100\% \times 0\% &= 0\% & (\mathbf{Det}_W, \mathbf{2})\text{-simulations with response} & \text{-/-/Alt/Null} \\
100\% \times 100\% &= 100\% & (\mathbf{Det}_W, \mathbf{2})\text{-simulations with response} & \text{-/-/Alt/Alt}
\end{aligned} \tag{18}$$

- Let us now consider a $(\mathbf{Sto}_W, \mathbf{1})$ process, among tests **i)** to **iv)**, only the first and the last one are led under the Null hypothesis. Consequently, when $\alpha = 5\%$, each of tests **i)** and **iv)** may approximately produce the **Null** response in 95% simulations, and the **Alt** response in the other 5%. This yields to the following theoretical percentages

$$\begin{aligned}
95\% \times 95\% &= 90.25\% & (\mathbf{Sto}_W, \mathbf{1})\text{-simulations with response} & \mathbf{Null/-/-/Null} \\
95\% \times 5\% &= 4.75\% & (\mathbf{Sto}_W, \mathbf{1})\text{-simulations with response} & \mathbf{Null/-/-/Alt} \\
5\% \times 95\% &= 4.75\% & (\mathbf{Sto}_W, \mathbf{1})\text{-simulations with response} & \mathbf{Alt/-/-/Null} \\
5\% \times 5\% &= 0.25\% & (\mathbf{Sto}_W, \mathbf{1})\text{-simulations with response} & \mathbf{Alt/-/-/Alt}
\end{aligned} \tag{19}$$

- Finally for $(\mathbf{Sto}_W, \mathbf{2})$ process, among tests **i)** to **iv)**, only the first and the second one are led under the Null hypothesis of the presence of an unit root. Let us point out that OPP test is very efficient to detect single unit roots, but it has not been developed to deal with the case of multiple unit roots. Consequently, OPP behavior in test **ii)**, *i.e.* on the differentiated series, which is nothing else than a $(\mathbf{Sto}_W, \mathbf{1})$ process, will be adequate and can be anticipated with proportion α for **Alt** response, and respectively $1 - \alpha$ for **Null**; while the answers given on the initial series will not necessarily be in adequacy with these proportions.

2.2.5.3. Higher degree trends. Actually, it is possible to detect higher-degree trends, either deterministic $(\mathbf{Det}, \mathbf{d})$ or stochastic $(\mathbf{Sto}, \mathbf{d})$, with $d = 3, 4, 5$, by iterating OPP and KPSS tests on the successive differentiated series. More precisely,

★ **Step 0 :**

Compute sample autocorrelation functions in order to distinguish between a white noise and a time series with a trend. If the series is driven by a trend, then run the following steps.

★ **Step 1 :**

Run OPP test on the given time series.

If the null is rejected, we identify a $(\mathbf{Det}, \mathbf{d})$ model, otherwise $(\mathbf{Sto}, \mathbf{d})$, with $d \geq 1$. It remains to precise d .

★ **Step 2 :**

Case 2a :

If a $(\mathbf{Sto}, \mathbf{d})$ model is detected in Step 1, differentiate the current time series, and apply OPP test. Iterate this step until the null is rejected. Then d corresponds to the number of necessary differentiations.

Case 2b :

If a $(\mathbf{Det}, \mathbf{d})$ model is detected in Step 1, differentiate the current time series, and apply KPSS test. Iterate this step until the null is not rejected. Then d corresponds to the number of necessary differentiations.

When applying this strategy, illustrated by a diagram in Figure D1, Appendix D, a model is suggested, leading either to Equation (1) or (2), with parameters to be determined. In particular, process $(B_t)_t$ is rarely a white noise, and should rather be modeled by an ARMA(p,q) process.

The validity of the global model has to be confirmed with residuals diagnosis.

2.2.6. Periodic trend

To deal with seasonal data, we assume that the season r is known and will be equal to 12, 4 or 2 for monthly, quarterly or biannual data respectively. In this case we follow the Box and Jenkins [3] approach:

- At the first step, we remove the seasonal component.
- In the second step, we apply our TDT strategy to the deseasonalized data.

In the first step one need to determine if the seasonal component is deterministic or stochastic, to consider the model (3) or (4). In [5] Canova and Hansen proposed the CH test where the null hypothesis is the presence of deterministic seasonal component whereas the alternative hypothesis is the presence of seasonal unit root. Hence we suggest to apply the CH test to the original data. If the null is not rejected, then we remove the seasonal component by using the harmonic regression to identify \mathbf{S}_t , in (3) and the deseasonalized data will be $Y_t = Z_t - \mathbf{S}_t$. If the null is rejected then the deseasonalized data will be $Y_t = (1 - L^r)Z_t$. We then apply our TDT strategy to Y_t .

3. Simulations

We ran 5 000 simulations using every data generating process among **(SN)**, **(Det,1)**, **(Det,2)**, **(Sto,1)** and **(Sto,2)**, as defined from Equation (6) to Equation (10). We set $n = 300$, $a_0 = 5$, $a_1 = 1$, $a_2 = 1$. Random generations of \mathcal{E}_t were taken from Gaussian centered variables with standard deviation $\sigma_{\mathcal{E}}$, a fixed value among $\{0.5, 1, 3, 5, 10, 20, 30, 50, 100, 200, 300, 500\}$, and the associated stationary noise is either a **(WN)**, or **(SN)** such as a MA(2) or an ARMA(1,1) centered, causal and invertible process. Details on simulations are given in Appendix, Section G.1.

3.1. Dickey-Fuller tests failure

Table 2 shows that Dickey-Fuller diagnosis is accurate for **(WN)** and **(Sto_W,1)** models. As expected, only the convenient model **(M₃)**, provides a correct answer for **(Det_W,1)**. And in Figure E1 from Appendix E, we illustrate that diagnosis is unclear for **(Det_W,1)** realizations when using any test under models **(M₁)** or **(M₂)**. Indeed, results vary greatly according to parameter $\sigma_{\mathcal{E}}$, taking value in the set $\{0.5, 1, 3, 5, 10, 20, 30, 50, 100, 200, 300, 500\}$. Surprisingly, unit root is far to be correctly detected in **(Sto_W,2)** realizations. Finally, diagnosis is mainly incorrect for model **(Det_W,2)**, since unit roots are systematically detected, whereas we have $\rho = 0$. Thus, Dickey-Fuller-based tests fail in diagnosing unit root for quadratic trends models.

Several strategies based on Dickey-Fuller tests have been developed ([10, 21, 12]). From Table 2, we can deduce that all the strategies permit to discriminate between first-order deterministic or stochastic trend, but they do not plan to integrate second-order trends. Thus, the most simple strategy proposed in [10] falsely classifies **(Det_W,2)** model as a random walk, whereas Perron predicts a linear-trend stationary process [21]. The most advanced strategy given in [12] nearly identifies **(Det_W,2)** processes, by describing them as $\Delta(Z_t) = \beta_0 + \beta_1 t + \mathcal{E}_t$, instead of $\Delta(Z_t) = \beta_0 + \beta_1 t + \Delta(\mathcal{E}_t)$, where $\Delta(Z_t) = Z_t - Z_{t-1}$ is the differentiated series. But diagnosis is mainly incorrect for **(Sto_W,2)** processes. Surprisingly, only the most simple strategy suggested in [10] detects unit root in half realizations, and predicts either a linear-trend stationary process or a stationary AR(1) process otherwise. And other strategies predict linear-trend stationary

Table 2.: Null-hypothesis rejection rate (%) in Dickey-Fuller tests, when $\sigma_{\mathcal{E}} = 10$.

Test	DGP ^a				
	(WN)	(Det _W ,1)	(Det _W ,2)	(Sto _W ,1)	(Sto _W ,2)
Test ρ under (M ₁)	100	0	0	5.06	0
Test ρ under (M ₂)	100	0	0	4.96	12.88
Test ρ under (M ₃)	100	100	0	5.04	32.4
Test Φ_1 under (M ₂)	100	0	100	4.86	95.46
Test Φ_2 under (M ₃)	100	100	100	4.92	99.08
Test Φ_3 under (M ₃)	100	100	100	5.1	90.4

^aData Generating Process.

Table 3.: Null-hypothesis rejection rate (%) for KPSS and OPP stationarity tests, for DGP simulations when the underlying process is a white noise $(\mathcal{E}_t)_t$. We vary $\sigma_{\mathcal{E}}$ on the set $\{0.5, 1, 3, 5, 10, 20, 30, 50, 100, 200, 300, 500\}$. The final rejection rate is computed as the average of the rejection rates obtained for each $\sigma_{\mathcal{E}}$.

Test	DGP ^a				
	(WN)	(Det _W ,1)	(Det _W ,2)	(Sto _W ,1)	(Sto _W ,2)
OPP for Z_t	100	100	100	5.96	0
OPP for $\Delta(Z_t)$	100	100	100	100	5.86
KPSS for Z_t	4.8	98.6	100	98.9	100
KPSS for $\Delta(Z_t)$	0	0	100	4.8	98.9

^aData Generating Process.

process. Consequently, it appears necessary to elaborate a new strategy to identify not only one-degree trends, but also higher-degree ones.

3.2. Accurate behavior for OPP and KPSS tests

Table 3 presents the null-hypothesis rejection rate when $B_t = \mathcal{E}_t$ where $\sigma_{\mathcal{E}}$ varies in $\{0.5, 1, 3, 5, 10, 20, 30, 50, 100, 200, 300, 500\}$. It shows that KPSS and OPP tests perform as expected, not only for simulations driven from one-order trends, but also for quadratic trends. Moreover, results remain identical for any value of parameter $\sigma_{\mathcal{E}}$, varying from 0.5 to 500, such as shown in Figure F1, Appendix F. We also present results for simulations with underlying stationary noises $(B_t)_t$, such as a MA(2) and an ARMA(1,1). In this case, both Figures G1 and G2, in Appendix Section G.2, show the same behavior for KPSS and OPP tests, whatever $\sigma_{\mathcal{E}}$ value.

3.3. TDT strategy

We applied successively tests **i)** to **iv)** to any simulation, using a risk $\alpha = 5\%$. In Table 4, every column returns the diagnosis percentage associated to the corresponding DGP. All the results with $\sigma_{\mathcal{E}}$ value in the set $\{0.5, 1, 3, 5, 10, 20, 30, 50, 100, 200, 300, 500\}$ are pooled, since the observed percentages show a very high stability with respect to $\sigma_{\mathcal{E}}$. As we have pointed out before, the percentage in bold refers to the theoretical diagnosis, *i.e* the responses given in equations (11)-(15). We observe that, even if alternative responses can be observed, the modal responses given by the TDT strategy are the theoretical ones.

Let us first consider simulations generated from a (WN) model, only two sets of responses were obtained to TDT : **Alt/Alt/Null/Null** for 95.25% of (WN) simulations (percentage written in bold), and **Alt/Alt/Alt/Null** for the other 4.75% simulations. This result is convenient with

the expected behavior of KPSS test, as described in Section 2.2.5.2, Equation (16), where the expected percentage is 95% (resp. 5%) for $-/-/\text{Null}/\text{Null}$ (resp. $-/-/\text{Alt}/\text{Null}$) response. The new element that appears thanks to the simulations is that OPP test is consistent for a stationary noise *i.e.* the power converges to one as $n \rightarrow +\infty$. As far as $(\text{Det}_W,1)$ or $(\text{Det}_W,2)$ processes are concerned, almost only the theoretical response was observed (99.99% and 100% resp.), which is in line with the expected results given in Equations (17) and (18). Once again, the novelty lies in the high power of the OPP test for series generated by a deterministic trend, as defined in Equation (1). Finally, for $(\text{Sto}_W,1)$ or $(\text{Sto}_W,2)$ simulations, more responses are observed, but they remain consistent with the expected results presented in Section 2.2.5.2. On the one hand, $(\text{Sto}_W,1)$ provides observed response rates very close to the expected ones, given in Equation (19). Indeed the observed percentage 89.38% (resp. 4.28%, 5.91% and 0.44%) for $\text{Null}/-/-/\text{Null}$ (resp. $\text{Null}/-/-/\text{Alt}$, $\text{Alt}/-/-/\text{Null}$ and $\text{Alt}/-/-/\text{Alt}$) response is very close to the expected one 90.25% (resp. 4.75%, 4.75% and 0.25%). This time, to compute the observed percentages, it is necessary to sum over the convenient associated responses. For instance, the 89.38% rate for the observed $\text{Null}/-/-/\text{Null}$ response is the sum of percentages 86.162% and 3.216% observed for $\text{Null}/\text{Alt}/\text{Null}/\text{Null}$ and $\text{Null}/\text{Null}/\text{Alt}/\text{Null}$ responses respectively. On the other hand $(\text{Sto}_W,2)$ simulations show that KPSS test has a high power on these series, detecting almost always the non-stationarity induced by a double unit root, and moreover that even if OPP test was not developed to deal with multiple unit root, it detects, in a too conservative way, the presence of this double unit root.

But the interest of Table 4 lies in its reverse reading. Let us associate a DGP to a TDT diagnosis. As an example, since none simulation under (WN) , $(\text{Det}_W,1)$, $(\text{Det}_W,2)$ or $(\text{Sto}_W,1)$ DGP led to responses $\text{Null}/\text{Null}/\text{Alt}/\text{Alt}$, then if one obtains such a response on its time series, this means that a $(\text{Sto}_W,2)$ model is suitable. Alternately $\text{Alt}/\text{Alt}/\text{Alt}/\text{Null}$ diagnosis could lead either to a (WN) , a $(\text{Det}_W,1)$ or a $(\text{Sto}_W,1)$ model. But referring to occurrence percentages, $99.993/(4.753 + 99.993 + 5.822) = 90.436\%$ of simulations with TDT $\text{Alt}/\text{Alt}/\text{Alt}/\text{Null}$ are produced by a $(\text{Det}_W,1)$ DGP, only 4.299% by a (WN) and 5.266% by a $(\text{Sto}_W,1)$. Then a $(\text{Det}_W,1)$ model appears as the best candidate, but (WN) and $(\text{Sto}_W,1)$ models can not be totally excluded. In this precise case, even if a linear trend is present, the relevance of either a (WN) or a $(\text{Det}_W,1)$ model depends on the intensity of the trend in relation to the variance of the associated noise. The convenient choice can be ruled out by previously computing autocorrelation functions. If several models remain acceptable, then we suggest to construct and compare them.

Let us remark that classification stability may decrease when $\sigma_{\mathcal{E}}$ keeps growing. Indeed when noise intensity becomes too high compared to the linear coefficient a_1 , the trend becomes imperceptible, and KPSS test may progressively fail to reject the null for several $(\text{Det}_W,1)$ simulations. Then the accurate response $\text{Alt}/\text{Alt}/\text{Alt}/\text{Null}$ may successively be replaced by the wrong response $\text{Alt}/\text{Alt}/\text{Null}/\text{Null}$, that is accurate for (WN) . And the confusion between $(\text{Det}_W,1)$ and (WN) naturally increases with $\sigma_{\mathcal{E}}$. But note that in this case, the true model $(\text{Det}_W,1)$ might no longer be the most suitable for the series, and a simple (WN) model should be preferred.

In order to evaluate the effect of autocorrelation on TDT strategy, we also run simulations with autocorrelated noises. In other words, we replaced \mathcal{E}_t either by a MA(2) process or by an ARMA(1,1) process, denoted as B_t , see Supplementary Section 1.3. Percentage of TDT diagnosis associated to every Data Generating Process, driven by (SN) , are given in Supplementary, in Tables S1 and S2. Percentage diagnosis remains similar regardless of the underlying model for B_t , and are still highly stable with respect to $\sigma_{\mathcal{E}}$ value. From Table 4 and Supplementary Tables S1 and S2, we suggest to associate each model with some sets of responses to TDT.

Finally, from Table 4 we observe that the five responses $\text{Alt}/\text{Alt}/\text{Null}/\text{Alt}$, $\text{Alt}/\text{Null}/\text{Alt}/\text{Alt}$, $\text{Alt}/\text{Null}/\text{Null}/\text{Alt}$, $\text{Alt}/\text{Null}/\text{Alt}/\text{Null}$ and $\text{Alt}/\text{Null}/\text{Null}/\text{Null}$ never appear as output of the TDT strategy, therefore we propose the following associations :

Table 4.: Percentage of Trend Diagnosis Tests (TDT) associated to every Data Generating Process (DGP) when σ_ε takes values in $\{0.5, 1, 3, 5, 10, 20, 30, 50, 100, 200, 300\}$.

TDT ^b	DGP ^a				
	(WN)	(Det _{W,1})	(Det _{W,2})	(Sto _{W,1})	(Sto _{W,2})
Alt/Alt/Alt/Alt	0	0	100^c	0.438	0
Alt/Alt/Null/Alt	0	0	0	0	0
Alt/Null/Alt/Alt	0	0	0	0	0
Alt/Null/Null/Alt	0	0	0	0	0
Null/Alt/Alt/Alt	0	0	0	4.273	6.213
Null/Alt/Null/Alt	0	0	0	0.005	0
Null/Null/Alt/Alt	0	0	0	0	90.427
Null/Null/Null/Alt	0	0	0	0	0.007
Alt/Alt/Alt/Null	4.753	99.993	0	5.822	0
Alt/Alt/Null/Null	95.247	0.007	0	0.084	0
Alt/Null/Alt/Null	0	0	0	0	0
Alt/Null/Null/Null	0	0	0	0	0
Null/Alt/Alt/Null	0	0	0	86.162	0.089
Null/Alt/Null/Null	0	0	0	3.216	0
Null/Null/Alt/Null	0	0	0	0	3.220
Null/Null/Null/Null	0	0	0	0	0.015
Total percentage	100	100	100	100	100

^aData Generating Process

^bTrend Diagnosis Tests

^cBold font highlights the expected TDT diagnosis associated to every DGP.

- Alt/Alt/Null/Null is associated with (SN) ,
- Alt/Alt/Alt/Null is associated with (Det,1) ,
- Alt/Alt/Alt/Alt is associated with (Det,2) ,
- Null/Alt/Alt/Null
Null/Alt/Null/Null
Null/Alt/Null/Alt are associated with (Sto,1) ,
- Null/Null/Alt/Alt
Null/Null/Alt/Null
Null/Null/Null/Alt
Null/Null/Null/Null are associated with (Sto,2) ,
- Null/Alt/Alt/Alt is associated either with (Sto,1) or (Sto,2) .

(20)

4. Application on data

4.0.1. Money Stock in USA

We consider money stock evolution in USA, that is given in Billions of Dollars and annual averaged from 1889 to 1988 (see Figure 3 - Left). Autocorrelation functions, given in Figure 3 (Right), confirm that data are driven by a trend.

Table H1 shows that our strategy TDT applied to money stock data suggests a (Sto,2)

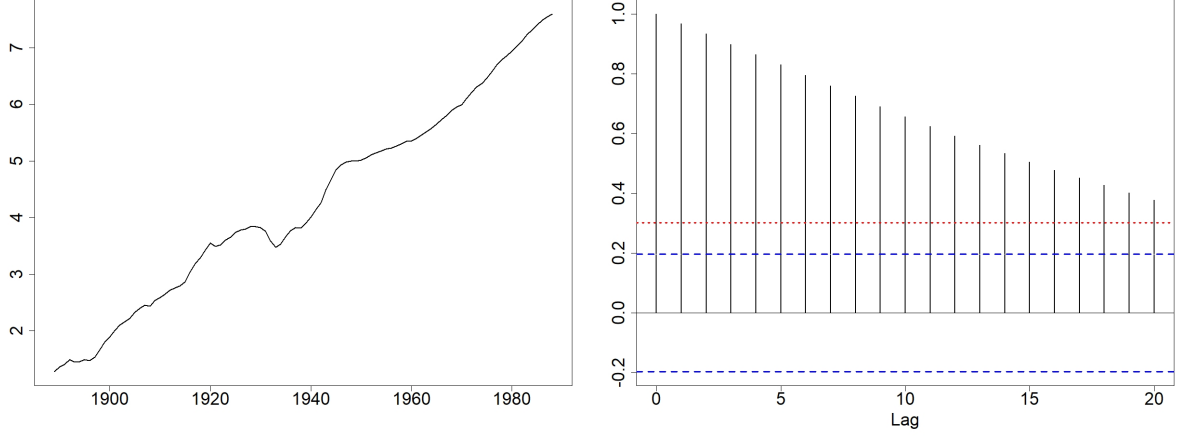


Figure 3.: Money stock data evolution (Left) and autocorrelation functions (Right).

Table 5.: p-values provided by several tests on the initial and the differentiated Money stock series.

Series	Test				
	OPP	KPSS	ρ under (M_1)	ρ under (M_2)	ρ under (M_3)
Z_t	0.2	0.01	0.99	0.99	0.94
$\Delta(Z_t)$	0.09	0.1	0.01	0.01	0.01

model. Dickey-Fuller tests rather suggest a **(Sto,1)** model. Indeed, most Dickey-Fuller tests do not reject the null for the initial series, but they are unable to detect a unit root in the differentiated series. We construct both a **(Sto,1)** and a **(Sto,2)** model, as in Equation (2), by modeling the stationary process $(B_t)_t$ by the first clearly valid model among all ARMA(p,q) with $p, q \leq 2$, sorted by minimizing Schwarz's Bayesian Criterion [24]:

- $(B_t)_t$ is MA(2) for **(Sto,2)** model, suggested by our strategy TDT.
- $(B_t)_t$ is ARMA(1,1) for **(Sto,1)** model, suggested by Dickey-Fuller tests.

In Table 6, we compare both models relevance in terms of prediction criteria computed between the observed series and predictions for the last 10 values(almost 10%), such as Root Mean Square Error (RMSE) and Mean Absolute Percentage Error (MAPE). Table 6 shows that the **(Sto,2)** model provided by our strategy is the most suitable. In Supplementary Section 2, we additionally explore the other American macroeconomic indexes contained in Nelson-Plosser data.

Table 6.: Models comparison for Money stock series.

Model	Criterion	
	RMSE	MAPE
TDT^a: (Sto,2) with MA(2)	0.038	0.362
DF^b: (Sto,1) with ARMA(1,1)	0.317	3.549

^aTrend Diagnosis Tests.

^bDickey-Fuller tests.

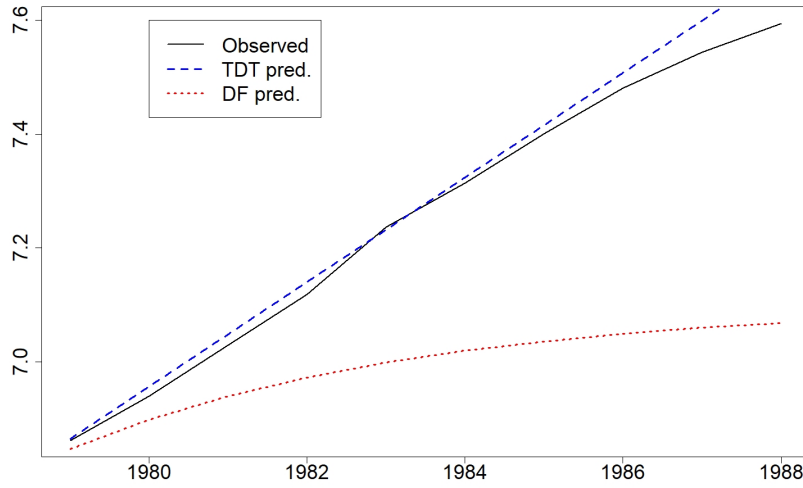


Figure 4.: Predictions for money stock series with TDT and DF models.

4.0.2. Evolution of atmospheric CO2 concentration

Since 1959, atmospheric CO2 concentration (ppm) has been measured monthly, at Mauna Loa Observatory, Hawaiï see [16]. Figure 5 reveals that the global average concentration of atmospheric carbon dioxide has a clear increasing trend, and also a seasonal monthly component.

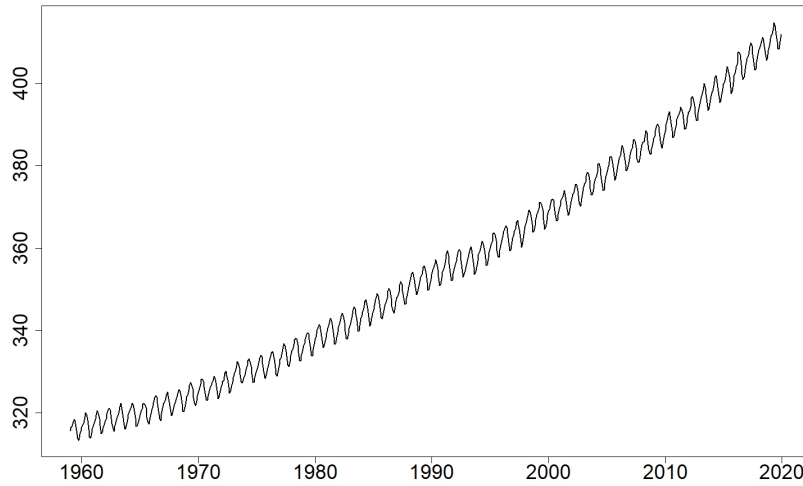


Figure 5.: CO2 atmospheric concentration evolution.

As described in Section 2.2.6, we start by removing the seasonal component. Since the data are given monthly, the underlying period is $r = 12$. CH-test indicates that the seasonality is deterministic (CH-test, p-value=1). Thus we deseasonalize, by regressing the CO2 series on the

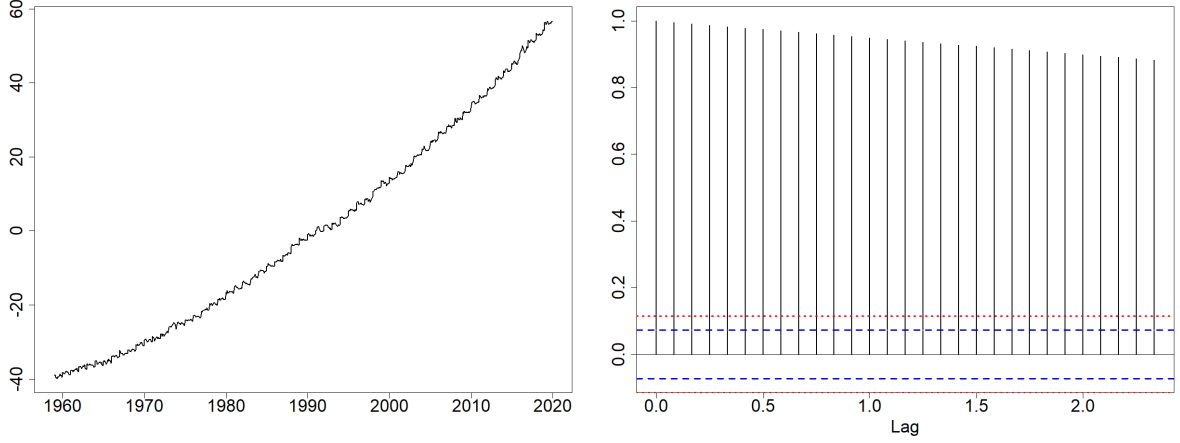


Figure 6.: CO2 deseasonalized series evolution (Left) and associated autocorrelation functions (Right).

Table 7.: p-values provided by several tests on CO2 deseasonalized series.

Series	Test				
	OPP	KPSS	ρ under (M_1)	ρ under (M_2)	ρ under (M_3)
Z_t	0.01	0.01	0.9791	0.99	0.5465
$\Delta(Z_t)$	0.01	0.01	0.01	0.01	0.01

seasonal dummy variables and by retaining the residuals from this regression. Autocorrelation functions plotted in Figure 6 (Right) show that the remaining series is driven by a trend. From Table 7, we see that Dickey-Fuller tests applied to the deseasonalized series clearly suggests a **(Sto,1)** model, whereas our TDT strategy produces responses **Alt/Alt/Alt/Alt** to tests **i)** to **iv)**, suggesting rather a **(Det,2)** model. We construct both a **(Sto,1)** and a **(Det,2)** model, as in Equations (1) and (2), by modeling the stationary process $(B_t)_t$ by the first valid model among all SARMA(p,q)(P,Q)[12] with $p, q, P, Q \leq 2$, sorted by minimizing Schwarz's Bayesian Criterion [24]:

- $(B_t)_t$ is SARMA(1,2)(1,1)[12] for **(Det,2)** model, suggested by our strategy TDT.
- $(B_t)_t$ is SARMA(1,0)(1,1)[12] for **(Sto,1)** model, suggested by Dickey-Fuller tests.

In Table 8, we compare both models relevance in terms of information criteria such as AIC, BIC, AICc [1, 24, 15] and prediction criterion computed between the observed series and predictions for the last six years (almost 10%), such as RMSE and MAPE. Table 8 shows that the **(Det,2)** model provided by our strategy is the most suitable.

Table 8.: Models comparison for CO2 deseasonalized series.

Model	Criterion	
	RMSE	MAPE
TDT ^a : (Det,2) with SARMA(1,2)(1,1)[12]	0.78	1.291
DF ^b : (Sto,1) with SARMA(1,0)(1,1)[12]	1.757	2.816

^aTrend Diagnosis Tests.

^bDickey-Fuller tests.

Figure 7 shows that forecasts for CO2 atmospheric concentration maintain the same trajectory, with great accuracy. Indeed, prediction intervals are so thin that they are hardly visible.

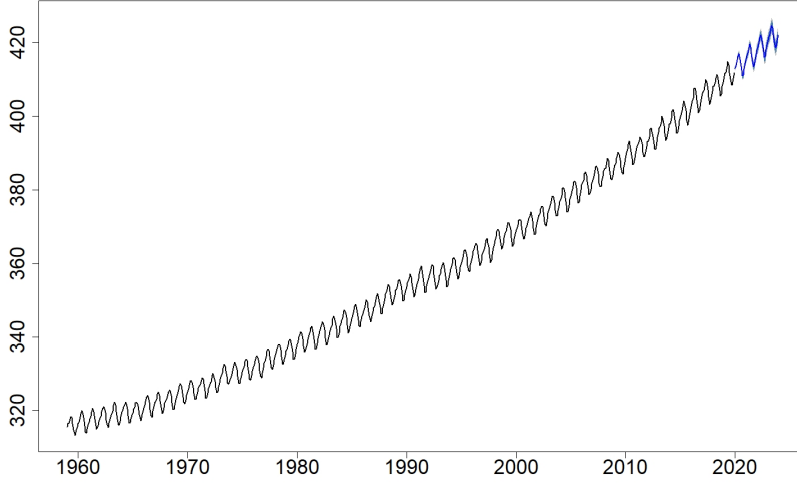


Figure 7.: Predictions for CO2 atmospheric concentration with TDT model, where prediction intervals colored in steel blue (resp. light grey) represent 80% (resp. 95%) confidence level.

5. Conclusion

We present a strategy to detect and identify the nature of the trend component in time series. We recall that, as a first analysis, visualizing time series plot is indispensable, since it may already suggest the presence of a trend. Then trend can be confirmed by analyzing autocorrelation functions. Next, whence a trend is detected, it remains to identify its nature. Indeed deterministic or stochastic trends do not produce the same forecasts.

We have shown that the Dickey-Fuller test is not suitable. For instance it detects the presence of spurious unit root for series generated under model $(\mathbf{Det}_W, \mathbf{2})$. In this paper, we rather propose a strategy based on OPP and KPSS tests, called TDT, in order to select between either a $(\mathbf{Det}, \mathbf{d})$ (*i.e.* a deterministic polynomial trend) or a $(\mathbf{Sto}, \mathbf{d})$ (*i.e.* a stochastic trend). We have given theoretical justifications on the expected results when applying our TDT strategy to data (Subsections 2.2.5.1 and 2.2.5.2). In particular, we had to study the asymptotic behavior of the KPSS test statistic when the required assumptions are not verified (either a non invertible moving average or the two alternatives $(\mathbf{Det}_W, \mathbf{1})$ and $(\mathbf{Det}_W, \mathbf{2})$). Next our TDT strategy was assessed on simulations. We have performed simulations by considering some particular cases of these models namely (\mathbf{WN}) (*i.e.* a white noise), $(\mathbf{Det}_W, \mathbf{1})$ (*i.e.* a deterministic linear trend), $(\mathbf{Det}_W, \mathbf{2})$ (*i.e.* a deterministic quadratic trend), $(\mathbf{Sto}_W, \mathbf{1})$ (*i.e.* a stochastic trend with a single unit root) and $(\mathbf{Sto}_W, \mathbf{2})$ (*i.e.* a stochastic trend with a double unit root). It appears that the results observed on the simulations (Table 4) correspond to the expected results. Moreover, the simulations allow us to discuss the power of the OPP test when it is applied under the alternative hypothesis, and confirm that KPSS test has a size distortion if the underlying model is a non invertible moving average, since it never rejects the null. We have also pointed out that KPSS test is consistent under the two alternatives $(\mathbf{Det}_W, \mathbf{1})$ and $(\mathbf{Det}_W, \mathbf{2})$, since it always rejects the null in this case.

Let us remark that both procedures, TDT strategy and Dickey-Fuller tests, may result in the same model suggestion. But diagnosis can be different, especially for time series with a quadratic trend, that reduces Dickey-Fuller tests reliability. Hence when both procedures suggest different models, both model candidates should be computed, validated and compared. Applied on two real data sets in Section 4, our automatic TDT strategy provides a better model than the one provided using the classical Dickey-Fuller tests. Thus we illustrated the superiority of our strategy on the Dickey-Fuller tests in selecting the best models which minimize the error of prediction criteria, such as the RMSE and the MAPE. Therefore we recommend to use our TDT strategy in modeling non stationary time series as a procedure to choose a candidate model with an accurate nature of the trend.

As a conclusion, applying our strategy on data allows to identify a candidate model, which must be validated and eventually compared with other potential models.

References

- [1] H. Akaike, *Information theory as an extension of the maximum likelihood principle*, Second International Symposium on Information Theory, B.N. Petrov and F. Csaki, eds., vol. 1557, Springer, Akademiai Kiado, Budapest, Hungary, 1973, pp. 30–32.
- [2] M. Boutahar, *Comparison of non-parametric and semi-parametric tests in detecting long memory*, Journal of Applied Statistics **36** (2009), no. 9, 945–972.
- [3] G.E.P. Box, G.M. Jenkins, and Reinsel G.C., *Time Series Analysis : Forecasting and Control*, Holden-Day, San Francisco, 1976, Third Edition.
- [4] P.J. Brockwell and R.A. Davis, *Time series : Theory and methods*, Springer-Verlag, New York, 1991, Second Edition.
- [5] F. Canova and Hansen B.E., *Are seasonal patterns constant over time ? a test for seasonal stability*, Journal of Business and Economic Statistics **13** (1995), no. 3, 237–252.
- [6] K.H. Chan, J.C. Hayya, and J.K. Ord, *A Note on Trend Removal Methods : The Case of Polynomial Regression versus Variate Differencing*, Econometrica **45** (1977), no. 3, 737–744.
- [7] N.H. Chan and C.Z. Wei, *Limiting distributions of least squares estimates of unstable autoregressive processes*, Ann. Statist. **16** (1988), no. 1, 367–401.
- [8] J.H. Conway and R.K. Guy, *The book of numbers*, Springer-Verlag, New-York, 1996.
- [9] Y.A. Davydov, *The invariance principle of stationary processes*, Theory of probability and its application **XV** (1970), no. 3, 487–498.
- [10] D.A. Dickey, W.R. Bell, and R.B. Miller, *Unit Roots in Time Series Models: Tests and Implications*, J. Am. Stat. Assoc. **40** (1986), no. 1, 12–26.
- [11] D.A. Dickey and W.A. Fuller, *Distribution of the Estimators for Autoregressive Time Series with a Unit Root*, J. Am. Stat. Assoc. **74** (1979), no. 366, 427–431.
- [12] J.J. Dolado, T. Jenkinson, and S. Sosvilla-Rivero, *Cointegration and unit roots*, J. Econ. Surv. **4** (1990), no. 3, 249–273.
- [13] C. Ertur, *Méthodologies de test de la racine unitaire*, Rapport de recherche, Laboratoire d’Analyses et de techniques économiques (LATEC), Université de Bourgogne, hal-01527262, 1998.
- [14] G.H. Hardy and E.M. Wright, *An introduction to the theory of numbers*, 4th with corrections ed., Springer-Verlag, Oxford, Clarendon Press, 1975.
- [15] C. M. Hurvich and C.-L. Tsai, *Bias of the corrected AIC criterion for underfitted regression and time series models*, Biometrika **78** (1991), no. 3, 499–509.
- [16] C.D. Keeling, S.C. Piper, R.B. Bacastow, M. Wahlen, T.P. Whorf, M. Heimann, and H.A. Meijer, *Exchanges of atmospheric co₂ and ¹³co₂ with the terrestrial biosphere and oceans from 1978 to 2000. i. global aspects*, SIO Reference Series **6** (2001), no. 1, 1–28.

- [17] D. Kwiatkowski, P.C.B. Phillips, P. Schmidt, and Y. Shin, *Testing the Null Hypothesis of Stationarity against the Alternative of a Unit Root*, Journal of Econometrics **54** (1992), no. 1-3, 159–178.
- [18] C.R. Nelson and H. Kang, *Spurious Periodicity in Inappropriately Detrended Time Series*, Econometrica **49** (1981), no. 3, 741–751.
- [19] C.R. Nelson and C. Plosser, *Trends and random walks in macroeconomics time series : some evidences and applications*, Journal of Monetary Economics **10** (1982), no. 2, 139–162.
- [20] S. Ouliaris, J.Y. Park, and P.C.B. Phillips, *Testing for a Unit Root in the Presence of a Maintained Trend*, Advances in Econometrics and Modeling, Kluwer Academic Publishers, Needham, MA, 1989.
- [21] P. Perron, *Trends and Random Walk in Macroeconomics Time Series : Further Evidence from a New Approach*, JEDC **12** (1988), no. 2-3, 297–332.
- [22] P.C.B. Phillips and P. Perron, *Testing for a unit root in time series regression*, Biometrika **75** (1988), no. 2, 335–346.
- [23] Y.V. Prokhorov, *Convergence of random processes and limit theorems in probability theory*, Theory Probab. Appl **1** (1956), no. 2, 157–214.
- [24] G.E. Schwartz, *Estimating the dimension of a model*, Ann. Stat. **6** (1978), no. 2, 461–464.

Appendix A. Sample autocorrelation functions behavior for (Det,d) models – Proof of Theorem 2.2

We consider the polynomial case with degree $d \geq 1$. Let us define as $S_j(n)$ the sum of the j -th power of the first n integers:

$$S_j(n) = \sum_{k=1}^n k^j.$$

From Faulhaber’s formula, detailed in [8], we know that

$$S_j(n) = \frac{n^{j+1}}{j+1} + \frac{1}{2}n^j + \frac{1}{j+1} \sum_{p=2}^j \mathcal{B}_p \binom{j+1}{p} n^{j-p+1}, \quad (\text{A1})$$

where \mathcal{B}_p are rational numbers called Bernoulli numbers.

Lemma A.1. *For any $j \in \mathbb{N}^*$, the sum of the j -th power of the first n integers, $S_j(n)$, is a $(j+1)$ -degree polynomial with leading coefficient $\frac{1}{j+1}$. More precisely,*

$$S_j(n) = \frac{n^{j+1}}{j+1} + o(n^{j+1}), \quad (\text{A2})$$

where $o(f)$ is one of the Landau symbols, as defined in [14], p. 7-8. $o(f)$ is called "little-O of f ", and expresses the convergence to 0 of a given function, when it is divided by f .

Then,

$$\overline{Z} = \frac{a_d}{d+1} n^d + o(n^d) + \overline{B}. \quad (\text{A3})$$

In order to study the asymptotic behavior of variables $\Xi(h)$, estimators of the theoretical auto-

correlation function for stationary square-integrable processes, we first compute variables $\Gamma(h)$, estimators of the theoretical autocovariance function $\text{cov}(Z_t, Z_{t+h})$.

Definition A.2. From random variables (Z_1, \dots, Z_n) , we define the autocovariance function as

$$\Gamma(h) = \frac{\sum_{k=1}^{n-h} (Z_{k+h} - \bar{Z})(Z_k - \bar{Z})}{n}, \quad |h| \leq n.$$

Using Equation (A3), we can express $\Gamma(h)$, by summing from $k = 1$ to $k = n - h$ the products of

$$Z_k - \bar{Z} = \sum_{j=0}^d a_j k^j - \frac{a_d}{d+1} n^d + o(n^d) + B_k - \bar{B}$$

with

$$Z_{k+h} - \bar{Z} = \sum_{j=0}^d a_j (k+h)^j - \frac{a_d}{d+1} n^d + o(n^d) + B_{k+h} - \bar{B}.$$

We have to study every term, and clarify its asymptotic behavior.

- a) First, we consider all product terms involving either \bar{B} or $\sum_{k=1}^{n-h} \frac{B_k}{n}$, or $\sum_{k=1}^{n-h} \frac{B_{k+h}}{n}$. Let us denote by T_a the sum of all these terms. Since $(B_t)_t$ is **(SN)** satisfying Hypotheses (H1) to (H3), then we can apply the weak law of large numbers for moving averages (see [4], Prop 6.3.10) and obtain

$$\bar{B} \xrightarrow[n \rightarrow +\infty]{\mathbb{P}} \mathbb{E}(B_1) = 0,$$

so do converge $\sum_{k=1}^{n-h} \frac{B_k}{n}$ and $\sum_{k=1}^{n-h} \frac{B_{k+h}}{n}$. Since \bar{B} , $\sum_{k=1}^{n-h} \frac{B_k}{n}$, or $\sum_{k=1}^{n-h} \frac{B_{k+h}}{n}$ do multiply either themselves or polynomials with degree $\leq d$, then these product terms converge \mathbb{P} to 0, as soon as they are divided by n^d .

$$T_a = o_{\mathbb{P}}(n^d) \tag{A4}$$

- b) Next, we study the behavior of the following terms :

$$\begin{aligned} T_{b,1} &= \sum_{k=1}^{n-h} \frac{B_k B_{k+h}}{n}, \\ T_{b,2} &= \sum_{k=1}^{n-h} \sum_{j=0}^d a_j \frac{k^j B_{k+h}}{n}, \\ T_{b,3} &= \sum_{k=1}^{n-h} \sum_{j=0}^d a_j \frac{(k+h)^j B_k}{n}. \end{aligned}$$

Applying again the weak law of large numbers for moving averages (see [4], Prop 7.3.5), we

obtain the \mathbb{P} -convergence of term $T_{b,1}$ to $\gamma_B(h)$, and then

$$T_{b,1} = o_{\mathbb{P}}(n^d)$$

On the other hand, we need Cauchy-Schwarz's inequality to study terms $T_{b,2}$ and $T_{b,3}$ in the same way. We get

$$\begin{aligned} T_{b,2} &= \sum_{j=0}^d a_j \sum_{k=1}^{n-h} \left(\frac{k^j}{\sqrt{n}} \times \frac{B_{k+h}}{\sqrt{n}} \right) \\ &\leq \sum_{j=0}^d a_j \left[\left(\sum_{k=1}^{n-h} \frac{k^{2j}}{n} \right)^{1/2} \times \left(\sum_{k=1}^{n-h} \frac{B_{k+h}^2}{n} \right)^{1/2} \right] \\ &\leq \left(\frac{n-h}{n} \sum_{k=1}^{n-h} \frac{B_{k+h}^2}{n-h} \right)^{1/2} \sum_{j=0}^d a_j \left(\frac{n^{2j}}{2j+1} + o(n^{2j}) \right)^{1/2}. \end{aligned}$$

The weak law of large numbers for moving averages and Prop 7.3.5 in [4] imply the \mathbb{P} -convergence of the left hand term to $\gamma_B(0)^{1/2} = \sigma_B$. In addition, the right hand term is $o(n^{d+1})$. Consequently,

$$T_b = T_{b,1} + T_{b,2} + T_{b,3} = o_{\mathbb{P}}(n^{d+1}) \quad (\text{A5})$$

- c) Let us denote by T_c all the product terms involving $o(n^d)$, not studied yet. From Equation (A1), we get that $o(n^d)$ multiplies polynomials with degree $\leq d$. Then all product terms converge to 0, as soon as they are divided by n^d . Consequently, we have

$$T_c = o(n^{2d}). \quad (\text{A6})$$

- d) It remains to specify terms with polynomial products, in order to explicit the leading coefficient. Let us consider

$$\begin{aligned} T_{d,1} &= \frac{a_d^2}{(d+1)^2} \frac{n-h}{n} n^{2d}, \\ T_{d,2} &= -\frac{a_d}{d+1} n^d \times \sum_{j=0}^d a_j \sum_{k=1}^{n-h} \frac{k^j}{n}, \\ T_{d,3} &= -\frac{a_d}{d+1} n^d \times \sum_{j=0}^d a_j \sum_{k=1}^{n-h} \frac{(k+h)^j}{n}, \\ T_{d,4} &= \sum_{k=1}^{n-h} \left(\sum_{i=0}^d a_i \frac{k^i}{\sqrt{n}} \times \sum_{j=0}^d a_j \frac{(k+h)^j}{\sqrt{n}} \right). \end{aligned}$$

All the terms $T_{d,1}$ to $T_{d,4}$ contain a leading term, associated to degree $2d$. There is nothing

to do for $T_{d,1}$. Equation (A2) provides

$$\begin{aligned} T_{d,2} &= -\frac{a_d}{d+1}n^d \times \sum_{j=0}^d a_j \left(\frac{n^j}{j+1} + o(n^j) \right) \\ &= -\frac{a_d^2}{(d+1)^2}n^{2d} + o(n^{2d}). \end{aligned}$$

We get the same formula for $T_{d,3}$. In addition, Equation (A2) also provides

$$\begin{aligned} T_{d,4} &= \sum_{i,j=0}^d \frac{a_i a_j}{n} \sum_{k=1}^{n-h} k^i (k+h)^j, \\ &= \frac{a_d^2}{2d+1}n^{2d} + o(n^{2d}). \end{aligned}$$

Finally,

$$\begin{aligned} T_d &= T_{d,1} + T_{d,2} + T_{d,3} + T_{d,4} \\ &= \left(\frac{a_d^2}{(d+1)^2} \frac{n-h}{n} - 2 \frac{a_d^2}{(d+1)^2} + \frac{a_d^2}{2d+1} \right) n^{2d} + o(n^{2d}) \end{aligned} \quad (\text{A7})$$

Adding Equations (A4) to (A7), we obtain

$$\Gamma(h) = \left(\frac{a_d^2}{(d+1)^2} \frac{n-h}{n} - 2 \frac{a_d^2}{(d+1)^2} + \frac{a_d^2}{2d+1} \right) n^{2d} + o_{\mathbb{P}}(n^{2d})$$

Finally since $a_d \neq 0$,

$$\begin{aligned} \Xi(h) &= \frac{\Gamma(h)}{\Gamma(0)} \\ &= \frac{\left(\frac{a_d^2}{(d+1)^2} \frac{n-h}{n} - 2 \frac{a_d^2}{(d+1)^2} + \frac{a_d^2}{2d+1} \right) n^{2d} + o_{\mathbb{P}}(n^{2d})}{\left(\frac{-a_d^2}{(d+1)^2} + \frac{a_d^2}{2d+1} \right) n^{2d} + o_{\mathbb{P}}(n^{2d})} \\ &\xrightarrow[n \rightarrow +\infty]{\mathbb{P}} 1. \end{aligned}$$

Appendix B. Sample autocorrelation functions behavior for (Sto,d) models – Proof of Theorem 2.3

We just give the proof for $d = 1$, since the general case can be deduced using the decomposition technique suggested in [7].

We first differentiate the initial series at a given lag h :

$$V_{k,h} = Z_k - Z_{k-h} = \sum_{j=0}^{h-1} B_{k-j}.$$

Let L denotes de lag operator i.e. $LX_t = X_{t-1}$, hence $V_{k,h}$ can be written as

$$V_{t,h} = A(L)B_t,$$

where A is the following polynomial

$$A(z) = 1 + z + \dots + z^{h-1}.$$

Since $B_t = \Psi(L)\mathcal{E}_t$, where $\Psi(z) = \sum_{j \in \mathbb{Z}} b_j z^j$, it follows that

$$V_{t,h} = A(L)\Psi(L)\mathcal{E}_t = V(L)\mathcal{E}_t,$$

where

$$V(z) = A(z)\Psi(z) = \sum_{j \in \mathbb{Z}} v_j z^j, \quad \text{with } v_j = \sum_{i=0}^{h-1} b_{j-i}.$$

Consequently the process $(V_{t,h})$ is also a moving average, by straightforward calculations we can show that $(V_{t,h})$ satisfies Hypotheses (H1) to (H3).

Let us set

$$\begin{aligned} B_n(t) &= \frac{1}{\sqrt{n}} \sum_{k=1}^{[nt]} B_k, \\ V_{n,h}(t) &= \frac{1}{\sqrt{n}} \sum_{k=1}^{[nt]} V_{k,h}, \quad \text{for all } t \in [0, 1], \end{aligned}$$

where $[x]$ is the integer part of x . Then using [2] and Theorem 2 in [9], we get the weak convergence :

$$\begin{aligned} B_n(\cdot) &\xrightarrow[n \rightarrow +\infty]{D[0,1]} \sqrt{2\pi f_B(0)}W, \\ V_{n,h}(\cdot) &\xrightarrow[n \rightarrow +\infty]{D[0,1]} \sqrt{2\pi f_V(0)}W, \end{aligned}$$

where $D[0, 1]$ is the set of càdlàg functions with Skorokhod topology, and where $(W_t)_t$ is a standard Brownian motion. Moreover f_B and f_V are the spectral densities associated to processes (B_t) and $(V_{t,h})$:

$$f_B(\lambda) = \frac{\sigma_{\mathcal{E}}^2}{2\pi} \left| \sum_{j \in \mathbb{Z}} b_j e^{ij\lambda} \right|^2 \tag{B1}$$

$$f_V(\lambda) = \frac{\sigma_{\mathcal{E}}^2}{2\pi} \left| A(e^{ij\lambda}) \sum_{j \in \mathbb{Z}} b_j e^{ij\lambda} \right|^2 \tag{B2}$$

We also define

$$Z_n(t) = Z_{[nt]} - \bar{Z}, \text{ such that } Z_n\left(\frac{k}{n}\right) = Z_k - \bar{Z}.$$

We recall that

$$\frac{1}{\sqrt{n}}Z_n(t) = B_n(t) - \frac{1}{n} \sum_{j=1}^n B_n\left(\frac{j}{n}\right),$$

Then by weak convergence continuity, we obtain that

$$\frac{1}{\sqrt{n}}Z_n(\cdot) \xrightarrow[n \rightarrow +\infty]{D[0,1]} \sqrt{2\pi f_B(0)} W_{1,\cdot},$$

with

$$W_{1,t} = \left(W_t - \int_0^1 W_s ds \right).$$

Autocorrelation function definition was given in Equation (5). We deduce that

$$\Xi(h) = 1 + \frac{\sum_{k=1}^{n-h} (Z_k - \bar{Z}) V_{k+h,h}}{\sum_{k=1}^n (Z_k - \bar{Z})^2} + O_{\mathbb{P}}\left(\frac{1}{n}\right).$$

Then,

$$\begin{aligned} n(\hat{\Xi}(h) - 1) &= n \frac{\sum_{k=1}^{n-h} (Z_k - \bar{Z}) V_{k+h,h}}{\sum_{k=1}^n (Z_k - \bar{Z})^2} + O_{\mathbb{P}}(1) \\ &= \frac{\sum_{k=1}^{n-h} \frac{Z_n\left(\frac{k}{n}\right)}{\sqrt{n}} \left(V_n\left(\frac{k+h}{n}\right) - V_n\left(\frac{k+h-1}{n}\right) \right)}{\frac{1}{n} \sum_{k=1}^n \left(\frac{Z_n\left(\frac{k}{n}\right)}{\sqrt{n}} \right)^2} + O_{\mathbb{P}}(1) \\ &\xrightarrow[n \rightarrow +\infty]{\mathcal{L}} \frac{\sqrt{2\pi f_V(0)}}{\sqrt{2\pi f_B(0)}} \frac{\int_0^1 W_{1,s} dW_s}{\int_0^1 W_{1,s}^2 ds} = |h| \frac{\int_0^1 W_{1,s} dW_s}{\int_0^1 W_{1,s}^2 ds}. \end{aligned}$$

Prokhorov theorem ([23]) permits to deduce that $n(\hat{\Xi}(h) - 1) = O_{\mathbb{P}}(1)$.

Appendix C. Complements on KPSS statistic behavior in several particular cases – Complements to Section 2.2.4

C.1. Non-invertible MA(1) process

Let $(\mathcal{E}_t)_t$ be a white noise. We consider the following process

$$u_t = a + \mathcal{E}_t - \mathcal{E}_{t-1},$$

where constant a can be equal to 0. Such process $(u_t)_t$ accounts for the differentiated series $(\Delta(Z_t))_t$ when $(Z_t)_t$ is either **(WN)** or **(Det_W,1)**. Let us note that $(u_t)_t$ is a non-invertible MA(1) process, that does not satisfy our condition (H3-b). Above all its spectral density is given by

$$f_u(\lambda) = \frac{\sigma_{\mathcal{E}}^2}{2\pi} |1 - e^{i\lambda}|^2, \forall \lambda \in \mathbb{R},$$

and hence

$$f_u(0) = 0. \quad (\text{C1})$$

When developing KPSS test in [17], the authors suppose conditions of Phillips and Perron [22] on the error term u_t , among these conditions the following one on the long run variance:

$$\sigma^2 = \lim_{n \rightarrow \infty} \frac{1}{n} \mathbb{E} \left(\left(\sum_{t=1}^n u_t \right)^2 \right) = 2\pi f_u(0) > 0,$$

where n is the sample size of time series u_t . But from Equation (C1) such condition is not satisfied for the non invertible MA(1) process. Thus the theoretical developments in [17] on the asymptotic distribution of the test statistic LM_n cannot be applied here. Nevertheless doing computations in this case provides

$$LM_n \xrightarrow[n \rightarrow \infty]{\mathbb{P}} 0. \quad (\text{C2})$$

As a direct consequence of Equation (C2) KPSS test will never reject the null hypothesis, as n tends to ∞ , for series $(\Delta(Z_t))_t$ when $(Z_t)_t$ is either **(WN)** or **(Det_W,1)**.

C.2. (Det_W,1) and (Det_W,2) processes

We consider a processes $(Z_t)_t$ generated either under a **(Det_W,1)** or a **(Det_W,2)** model. Then the theoretical developments in [17] on the asymptotic distribution of the test statistic LM_n cannot be applied, since $(Z_t)_t$ is generated under the alternative hypothesis. Nevertheless doing computations in these cases provides

$$LM_n \equiv n^3, \text{ as } n \rightarrow \infty,$$

where symbol \equiv stands for the equivalence relation. Hence

$$LM_n \xrightarrow[n \rightarrow \infty]{\mathbb{P}} \infty. \quad (\text{C3})$$

As a direct consequence of Equation (C3) KPSS test will always reject the null hypothesis, as n tends to ∞ , for series $(Z_t)_t$ under either a **(Det_W,1)** or a **(Det_W,2)** model. Moreover this convergence remains valid if we consider the differentiated series $(\Delta(Z_t))_t$ when $(Z_t)_t$ is generated under a **(Det_W,2)** model, even if the associated noise becomes a non-invertible MA(1) process. This implies that KPSS test is powerful in all of these cases.

Appendix D. Diagram for high degree trends – Complement to Paragraph 2.2.5.3

We illustrate the strategy introduced in Paragraph 2.2.5.3, by a diagram. In addition, we indicate the R commands to use at the main steps. Note that the global approach is automated and implemented in our R-function *trend.diag.high()*, whose script can be found on our web page

www.i2m.univ-amu.fr/perso/manuela.royer-carezzi/AnnexesR.TrendTS/TrendTS.html

Appendix E. Boxplot of null-hypothesis rejection rate when σ_ε varies – Complement to Table 2

In the main paper, Table 2 shows results for $\sigma_\varepsilon = 10$. Here, Figure E1 displays results when all the simulations with σ_ε taking successive values in $\{0.5, 1, 3, 5, 10, 20, 30, 50, 100, 200, 300, 500\}$ are gathered. This illustrates the stability of Dickey-Fuller-testing response, as σ_ε varies, for most data generating process, except for **(Det_W,1)** simulations, showing high variability.

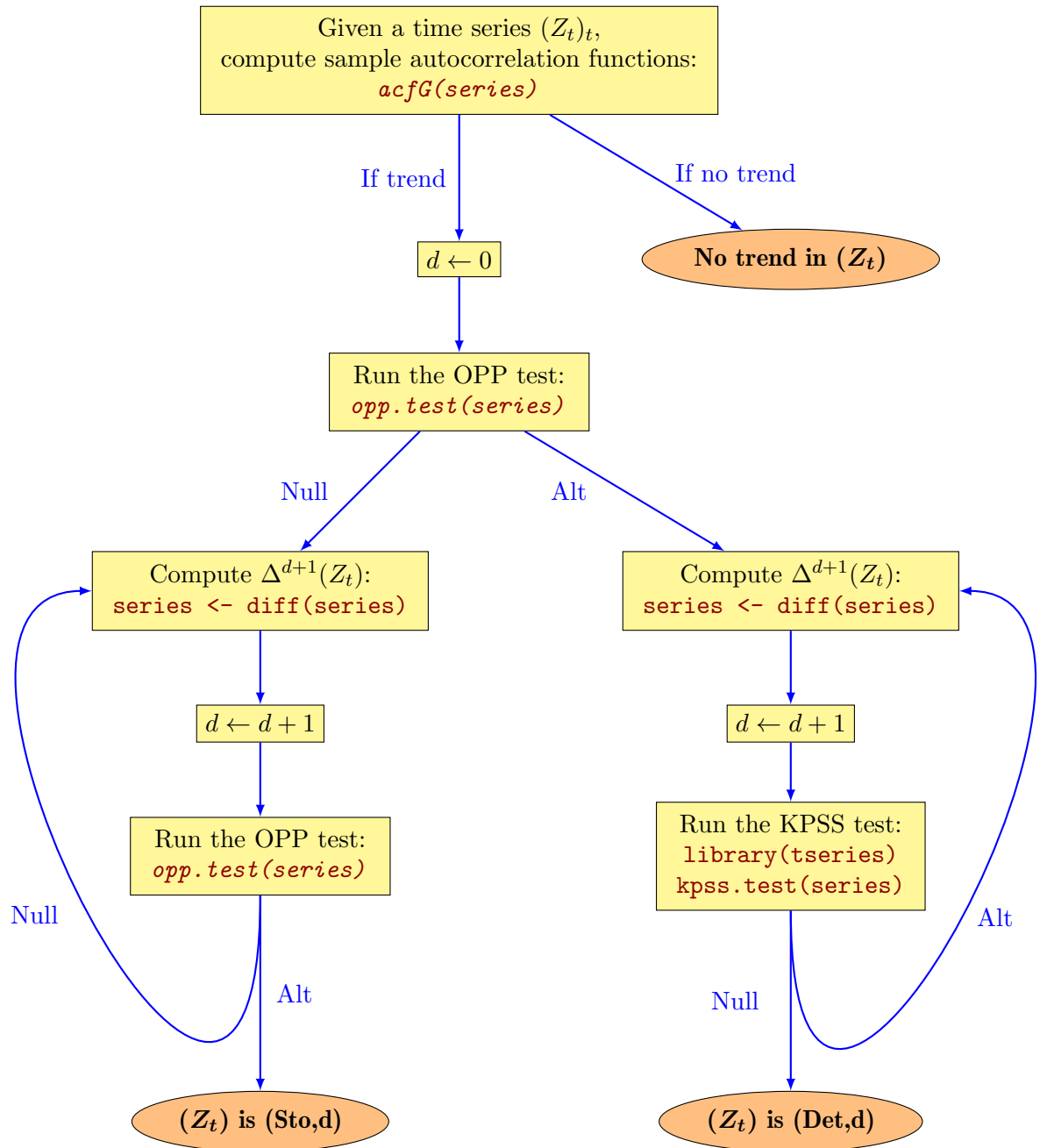


Figure D1.: TDT Strategy for high degree trends. Italic R-functions are available on our web page.

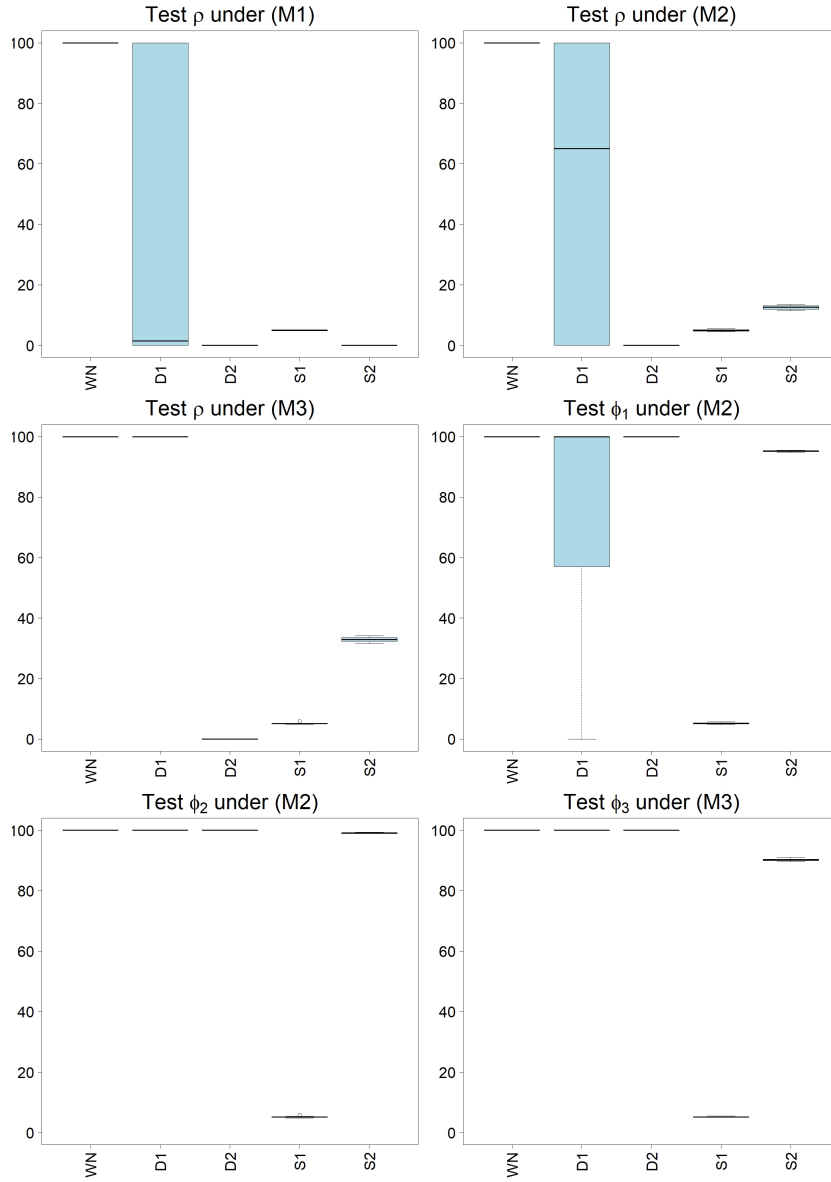


Figure E1.: Null hypothesis rejection rate for Dickey-Fuller tests, with respect to the underlying generating process used for simulations. All the simulations with $\sigma_{\mathcal{E}}$ taking successive values in $\{0.5, 1, 3, 5, 10, 20, 30, 50, 100, 200, 300, 500\}$ are gathered.

Appendix F. Boxplot of null-hypothesis rejection rate when $\sigma_{\mathcal{E}}$ varies, and when noise is (WN) – Complement to Table 3

In the main paper, Table 3 shows that KPSS and OPP tests perform accurately on (WN), (**Det_W,1**), (**Det_W,2**), (**Sto_W,1**) and (**Sto_W,2**) simulations. In Table, 3, $\sigma_{\mathcal{E}}$ successively takes values in the set $\{0.5, 1, 3, 5, 10, 20, 30, 50, 100, 200, 300, 500\}$ and the final rejection rate is computed by gathering all the simulations obtained for each $\sigma_{\mathcal{E}}$. Here, Figure F1 illustrates the stability of testing procedure for every data generating process as $\sigma_{\mathcal{E}}$ varies. Note that an outlier is observed when applying KPSS test to (**Det,1**) simulations. This means that KPSS test generally rejects the null hypothesis, as expected, in almost all cases. Actually, KPSS test sometimes fails to reject the null for several (**Det,1**) simulations with $\sigma_{\mathcal{E}} = 500$, that is to say when noise intensity is too high in relation to the linear coefficient a_1 , so that the trend becomes imperceptible. Thus $\sigma_{\mathcal{E}} = 500$ is above the high-limit for noise intensity.

Appendix G. Simulations

G.1. Details on simulations

We recall that we defined two trend types :

$$\text{Deterministic trend (Det,d)} \quad Z_t = a_0 + a_1 t + \dots + a_d t^d + B_t \quad (\text{G1})$$

$$\text{Stochastic trend (Sto,d)} \quad \Delta^d(Z_t) = B_t, \quad (\text{G2})$$

where we take $a_d \neq 0$, Δ is the 1-lag difference operator and $(B_t)_t$ is a \mathcal{L}^2 -integrable, centered, stationary process, denoted as (SN), for *Stationary Noise*. When $(B_t)_t$ is merely a sequence of identically distributed and independent centered variables, it is called (WN) for *White Noise* and denoted by $(\mathcal{E}_t)_t$. In this case, the associated models defined in Equations (G1) and (G2), are referred as (**Det_W,d**) and (**Sto_W,d**).

In the main paper, we study processes constructed with an underlying white noise process, denoted as (WN). Actually, we simulate random independent centered gaussian variables $(\mathcal{E}_t)_t$ with a standard deviation $\sigma_{\mathcal{E}}$, taking value in $\{0.5, 1, 3, 5, 10, 20, 30, 50, 100, 200, 300, 500\}$. Next we construct the related processes (**Det_W,1**), (**Det_W,2**), (**Sto_W,1**) and (**Sto_W,2**). But in the Supplementary, we also analyze simulations with an underlying stationary noise, that can be a causal, invertible ARMA process. Thus we consider either simulations from a MA(2) process

$$B_t = \mathcal{E}_t + \frac{1}{2}\mathcal{E}_{t-1} - \frac{1}{5}\mathcal{E}_{t-2}, \quad (\text{G3})$$

or an ARMA(1,1) process

$$B_t - \frac{1}{2}B_{t-1} = \mathcal{E}_t - \frac{1}{3}\mathcal{E}_{t-1}. \quad (\text{G4})$$

And we deduce the associated (**Det,1**), (**Det,2**), (**Sto,1**) and (**Sto,2**) processes. In details, we perform the following steps :

- 1) fix a value for $\sigma_{\mathcal{E}}$ among $\{0.5, 1, 3, 5, 10, 20, 30, 50, 100, 200, 300, 500\}$.
- 2) simulate B_t as either
 - a) $n = 300$ independent realizations of $\mathcal{N}(0, \sigma_{\mathcal{E}}^2)$
 - b) or $n = 300$ realizations of MA(2) process, defined in Equation (G3)

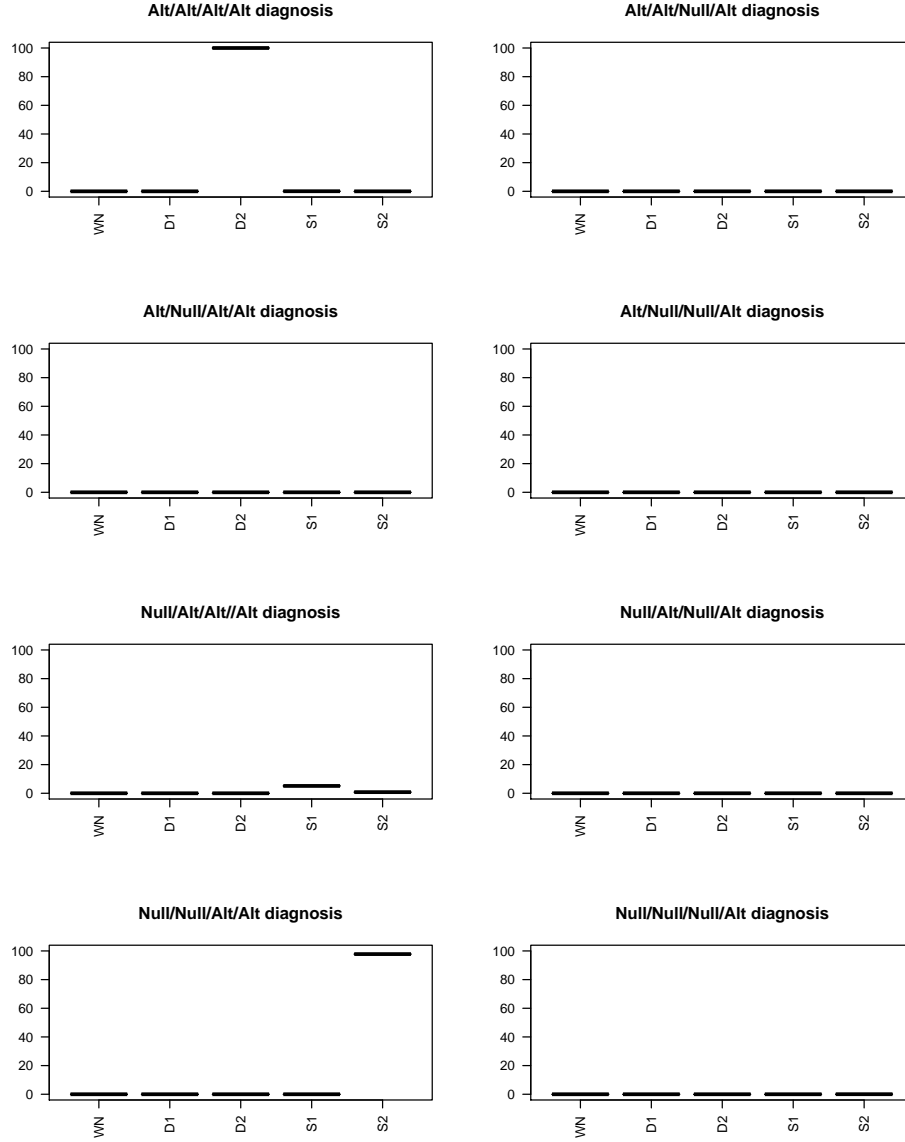


Figure F1.: Null hypothesis rejection rate for either KPSS or OPP stationarity tests applied upon either the initial or the differentiated series, with respect to the underlying generating process used for simulations. All the simulations, driven with a (**WN**), where $\sigma_{\mathcal{E}}$ takes successive values in $\{0.5, 1, 3, 5, 10, 20, 30, 50, 100, 200, 300, 500\}$, are gathered.

- c) or $n = 300$ realizations of ARMA(1,1) process, defined in Equation (G4)
- 3) construct the related processes
- (SN) = B_t
 - (Det,1) = $5 + t + B_t$
 - (Det,2) = $5 + t + t^2 + B_t$
 - (Sto,1) = Z_t such that $\Delta(Z_t) = B_t$
 - (Sto,2) = Z_t such that $\Delta^2(Z_t) = B_t$
- 4) run the stationarity test for every model process, generated in step 3) and compare the p-values with the nominal level $\alpha = 5\%$.

We repeat steps 2) to 4) 5000 times. And we repeat the whole procedure, as σ_ε successively takes values in $\{0.5, 1, 3, 5, 10, 20, 30, 50, 100, 200, 300, 500\}$.

We recall that all the functions are implemented in **R** language, and they are available at the website:

www.i2m.univ-amu.fr/perso/manuela.royer-carezzi/AnnexesR.TrendTS/TrendTS.html

In this page, we called

- Function `acfG.R` the R-code for sample autocorrelation plots with Sidak correction and binomial exact test, as explained in the main paper, Section 2.1, and a script `Example of acfG use` to detail its use,
- Function `opp.test.R` the R-code for OPP test, and a script `Example of opp.test use` to detail its use,
- Function `trend.diag.tests.R` the code for TDT strategy, as explained in the main paper in Section 3.3, and its associated script `Example of trend.diag.tests use`,
- Function `trend.diag.high.R` the code for TDT strategy, generalized for higher degree trends, as introduced in Paragraph 2.2.5.3, and its associated script `Example of trend.diag.high use`,
- Script `Tables2and3.R` the R-script to generate the simulations providing Table 2 , Table 3 and Figure F1 in the main paper, such as Figure ?? and Figure ?? in the Supplementary,
- Script `Table4.R` the R-script to generate the simulations providing Table 4 in the main paper, such as Table G1 and Table G2 in the Supplementary.

G.2. Behavior of KPSS and OPP stationarity tests when the underlying noise is not (WN) – Complement to Table 3 and Figure F1

In the main paper, Table 3 and Figure F1 show that KPSS and OPP tests perform accurately on (WN), (Det_W,1), (Det_W,2), (Sto_W,1) and (Sto_W,2) simulations. Now we consider simulations with an underlying stationary noise, denoted as B_t , that is a causal, invertible ARMA(p,q) process. Figure G1 (respectively Figure G2) displays results when $(B_t)_t$ follows a MA(2) (resp. ARMA(1,1)), as defined in Equation (G3) (resp. Equation (G4)). We set that σ_ε successively takes values in $\{0.5, 1, 3, 5, 10, 20, 30, 50, 100, 200, 300, 500\}$. We still observe the same convenient behavior, whatever $(B_t)_t$.

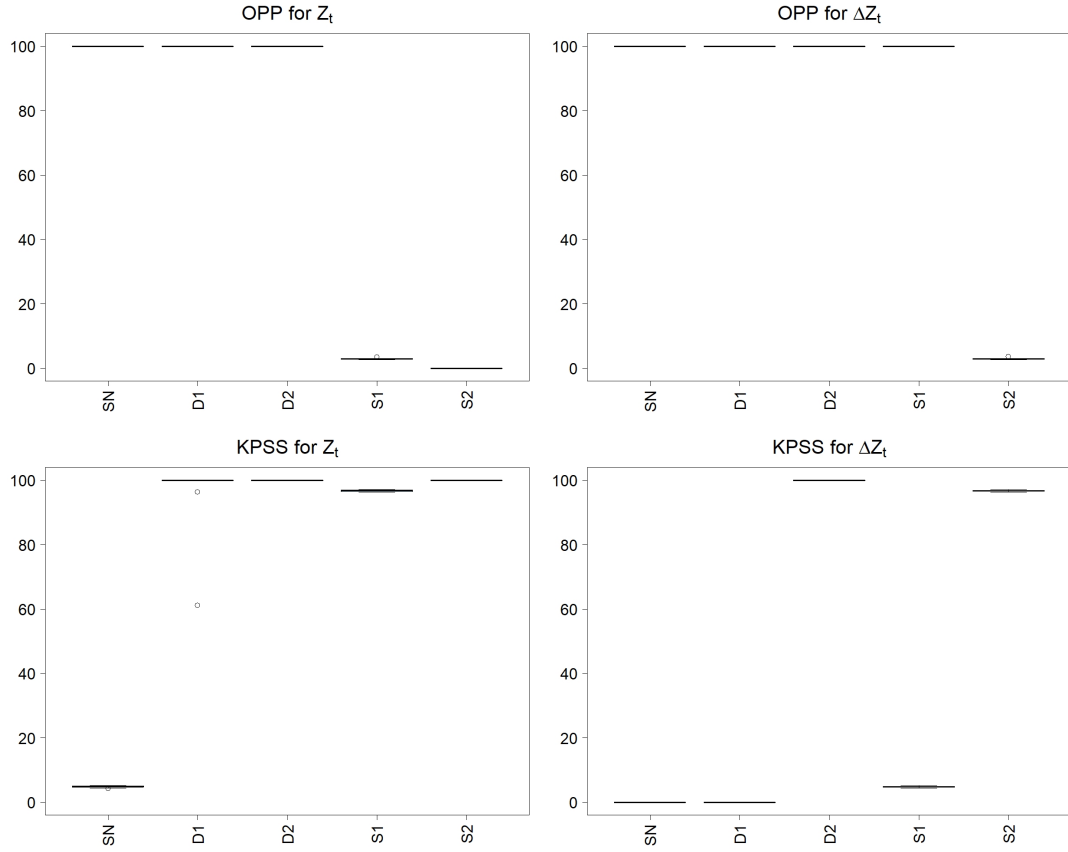


Figure G1.: Null hypothesis rejection rate for either KPSS or OPP stationarity tests applied upon either the initial or the differentiated series, with respect to the underlying generating process used for simulations. All the simulations, driven with a MA(2), where $\sigma_{\mathcal{E}}$ takes successive values in $\{0.5, 1, 3, 5, 10, 20, 30, 50, 100, 200, 300, 500\}$, are gathered.

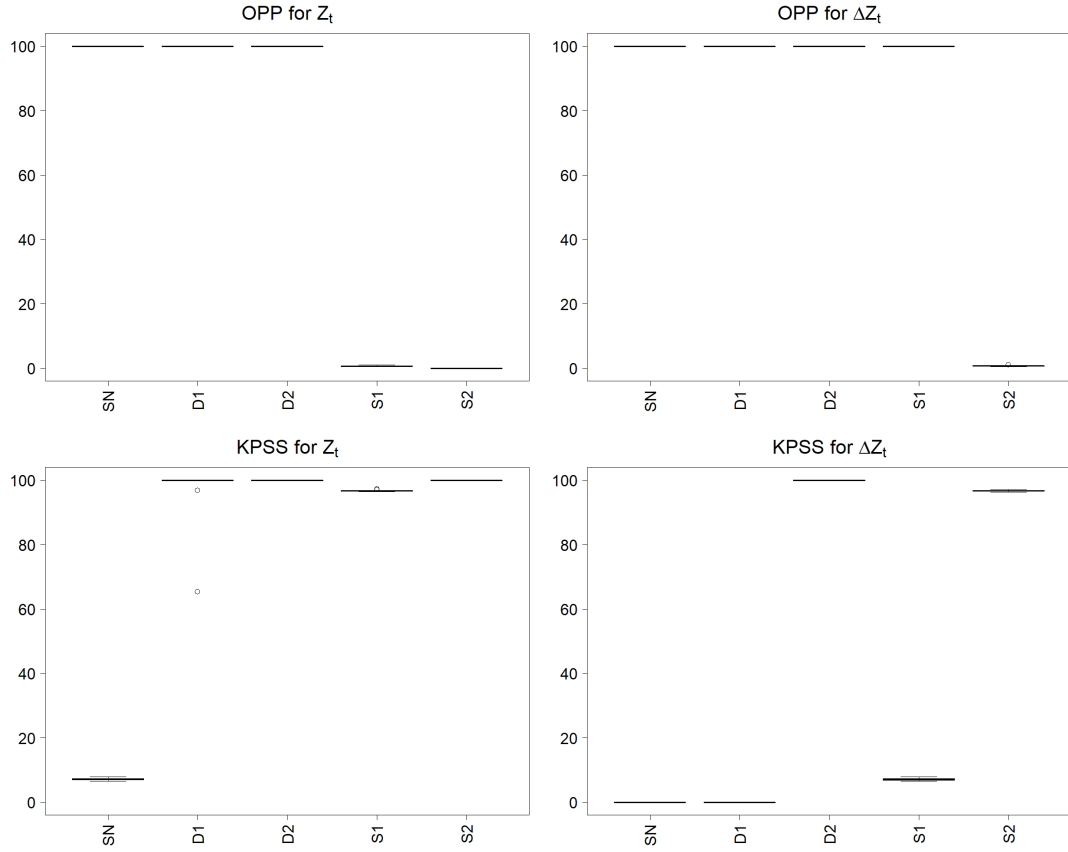


Figure G2.: Null hypothesis rejection rate for either KPSS or OPP stationarity tests applied upon either the initial or the differentiated series, with respect to the underlying generating process used for simulations. All the simulations, driven with a ARMA(1,1), where $\sigma_{\mathcal{E}}$ takes successive values in $\{0.5, 1, 3, 5, 10, 20, 30, 50, 100, 200, 300, 500\}$, are gathered.

G.3. Stability of diagnosis classification, when the underlying noise is not (WN)
– Complement to Table 4

In order to identify the trend nature of a time series $(Z_t)_t$, we suggest to apply the following tests successively :

- i)** OPP test to series Z_t ;
- ii)** OPP test to series $\Delta(Z_t)$;
- iii)** KPSS test to series Z_t ;
- iv)** KPSS test to series $\Delta(Z_t)$.

Under a rejection risk $\alpha = 5\%$, we denote by **Null**, the case where the null hypothesis can not be rejected, and by **Alt** otherwise. So that any time series can be associated to a single classification among the 2^4 possibilities. We call Trend Diagnosis Tests (TDT) the set of responses to tests **i)** to **iv)** computed on a time series.

In the main paper, Table 4 shows results for simulations driven by a white noise (**WN**), denoted as $(\mathcal{E}_t)_t$. The classification remains stable when $\sigma_{\mathcal{E}}$ keeps growing. But when noise intensity is too high in relation to the linear coefficient a_1 , the trend becomes imperceptible, and KPSS test sometimes fails to reject the null for several (**detT,1**) simulations with $\sigma_{\mathcal{E}} > 300$. Whereas **Alt/Alt/Alt/Null** diagnosis is accurately associated to almost 99.9% of (**detT,1**) simulations while $\sigma_{\mathcal{E}} \leq 300$, 83.6% of (**Det_W,1**) simulations with $\sigma_{\mathcal{E}} = 500$ have the convenient diagnosis **Alt/Alt/Alt/Null**, but the 16.4% other simulations are associated to diagnosis **Alt/Alt/Null/Null**, that is accurate for (**WN**). And the confusion between (**Det_W,1**) and (**WN**) naturally increases with $\sigma_{\mathcal{E}}$. In this case, the true model (**Det_W,1**) might no longer be the most suitable for the series.

Here, we consider simulations associated to a more general noise (**SN**), denoted as B_t , that is a causal, invertible ARMA(p,q) process. Table G1 (respectively Table G2) displays results when $(B_t)_t$ follows a MA(2) (resp. ARMA(1,1)), as defined in Equation (G3) (resp. Equation (G4)), when $\sigma_{\mathcal{E}}$ takes values in the set $\{0.5, 1, 3, 5, 10, 20, 30, 50, 100, 200, 300\}$. Furthermore Figures S3 and S4 illustrate the stability of the classification associated to every model as $\sigma_{\mathcal{E}}$ varies.

Table G1.: Percentage of Trend Diagnosis Tests (TDT) associated to every Data Generating Process (DGP). Simulations are driven with a MA(2), when σ_{ε} takes values in $\{0.5, 1, 3, 5, 10, 20, 30, 50, 100, 200, 300\}$.

TDT ^b	DGP ^a				
	(SN)	(Det,1)	(Det,2)	(Sto,1)	(Sto,2)
Alt/Alt/Alt/Alt	0	0	100^c	0.178	0
Alt/Alt/Null/Alt	0	0	0	0	0
Alt/Null/Alt/Alt	0	0	0	0	0
Alt/Null/Null/Alt	0	0	0	0	0
Null/Alt/Alt/Alt	0	0	0	4.562	3.131
Null/Alt/Null/Alt	0	0	0	0.005	0.002
Null/Null/Alt/Alt	0	0	0	0	93.463
Null/Null/Null/Alt	0	0	0	0	0.033
Alt/Alt/Alt/Null	4.744	99.638	0	2.940	0
Alt/Alt/Null/Null	95.256	0.362	0	0.040	0
Alt/Null/Alt/Null	0	0	0	0	0
Alt/Null/Null/Null	0	0	0	0	0
Null/Alt/Alt/Null	0	0	0	88.986	0.044
Null/Alt/Null/Null	0	0	0	3.289	0
Null/Null/Alt/Null	0	0	0	0	3.313
Null/Null/Null/Null	0	0	0	0	0.014
Total percentage	100	100	100	100	100

^aData Generating Process

^bTrend Diagnosis Tests

^cBold font highlights the expected TDT diagnosis associated to every DGP.

Table G2.: Percentage of Trend Diagnosis Tests (TDT) associated to every Data Generating Process (DGP). Simulations are driven with a ARMA(1,1), when σ_{ε} takes values in $\{0.5, 1, 3, 5, 10, 20, 30, 50, 100, 200, 300\}$.

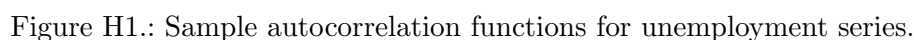
TDT ^b	DGP ^a				
	(SN)	(Det,1)	(Det,2)	(Sto,1)	(Sto,2)
Alt/Alt/Alt/Alt	0	0	100^c	0.085	0
Alt/Alt/Null/Alt	0	0	0	0	0
Alt/Null/Alt/Alt	0	0	0	0	0
Alt/Null/Null/Alt	0	0	0	0	0
Null/Alt/Alt/Alt	0	0	0	6.747	0.698
Null/Alt/Null/Alt	0	0	0	0.007	0
Null/Null/Alt/Alt	0	0	0	0	96.118
Null/Null/Null/Alt	0	0	0	0	0.029
Alt/Alt/Alt/Null	6.809	99.651	0	0.611	0
Alt/Alt/Null/Null	93.191	0.349	0	0.014	0
Alt/Null/Alt/Null	0	0	0	0	0
Alt/Null/Null/Null	0	0	0	0	0
Null/Alt/Alt/Null	0	0	0	89.465	0.011
Null/Alt/Null/Null	0	0	0	3.071	0
Null/Null/Alt/Null	0	0	0	0	3.124
Null/Null/Null/Null	0	0	0	0	0.020
Total percentage	100	100	100	100	100

^aData Generating Process

^bTrend Diagnosis Tests

^cBold font highlights the expected TDT diagnosis associated to every DGP.

In the main paper, we studied the *money stock* series from the macroeconomic Nelson-Plosser data. Actually, we applied our strategy on whole the 14 American macroeconomic indexes, contained in `tseries` R-package. Let us first study the *unemployment rate* series. Sample autocorrelation functions, plotted in Figure H1 do not show the typical behavior associated to series with a trend. Consequently, it should be modeled with a (SN) model.



37

Table H1.: p-values provided by several tests on the initial and the differentiated Nelson-Plosser series.

Series	Test				
cpi	OPP	KPSS	ρ under (M_1)	ρ under (M_2)	ρ under (M_3)
Z_t	0.2	0.01	0.99	0.99	0.99
$\Delta(Z_t)$	0.01	0.038	0.01	0.01	0.01
ip					
Z_t	0.17	0.01	0.99	0.727	0.084
$\Delta(Z_t)$	0.01	0.1	0.01	0.01	0.01
gnp.nom					
Z_t	0.2	0.01	0.99	0.99	0.912
$\Delta(Z_t)$	0.037	0.1	0.01	0.01	0.01
vel					
Z_t	0.2	0.01	0.012	0.084	0.741
$\Delta(Z_t)$	0.01	0.042	0.01	0.01	0.01
emp					
Z_t	0.2	0.01	0.99	0.894	0.436
$\Delta(Z_t)$	0.01	0.1	0.01	0.01	0.01
int.rate					
Z_t	0.2	0.01	0.84	0.861	0.833
$\Delta(Z_t)$	0.01	0.1	0.01	0.01	0.01
nom.wages					
Z_t	0.2	0.01	0.99	0.99	0.853
$\Delta(Z_t)$	0.03	0.1	0.01	0.01	0.01
gnp.def					
Z_t	0.2	0.01	0.99	0.99	0.952
$\Delta(Z_t)$	0.01	0.055	0.01	0.01	0.01
money.stock					
Z_t	0.2	0.01	0.99	0.99	0.943
$\Delta(Z_t)$	0.09	0.1	0.01	0.01	0.01
gnp.real					
Z_t	0.2	0.01	0.99	0.964	0.412
$\Delta(Z_t)$	0.012	0.1	0.01	0.01	0.01
stock.prices					
Z_t	0.2	0.01	0.99	0.99	0.653
$\Delta(Z_t)$	0.01	0.1	0.01	0.01	0.01
gnp.capita					
Z_t	0.2	0.01	0.99	0.953	0.371
$\Delta(Z_t)$	0.011	0.1	0.01	0.01	0.01
real.wages					
Z_t	0.2	0.01	0.99	0.679	0.938
$\Delta(Z_t)$	0.01	0.1	0.01	0.01	0.01